BAREKENG: Journal of Mathematics and Its Applications
December 2026 Volume 20 Issue 4 Page 3281-3304
P-ISSN: 1978-7227 E-ISSN: 2615-3017
https://doi.org/10.30598/barekengvol20iss4pp3281-3304

MATHEMATICAL MODELLING AND OPTIMAL CONTROL ANALYSIS OF TRIPLE-INTERVENTION STRATEGIES FOR SCHISTOSOMIASIS MANAGEMENT IN ENDEMIC REGIONS

Ayodeji Sunday Afolabi [1*], **Josiah Chukwuebuka Orji** [2]

[1,2]*Department of Mathematical Sciences, Federal University of Technology Akure, P.M.B. 704, Nigeria*

*Corresponding author's e-mail: * **asafolabi@futa.edu.ng***

Article Info

Article History:

Received: 13th October 2025
Revised: 28th April 2026
Accepted: 08th June 2026
Available online: 01st July 2026

Keywords:

Cercariae;
Mass drug administration;
Miracidia;
Molluscicide;
Optimal control;
Schistosomiasis;
Sensitivity analysis;
Stability analysis.

ABSTRACT

Schistosomiasis remains a significant public health challenge, affecting approximately 250 million people globally, particularly in endemic regions of sub-Saharan Africa. The disease is sustained through a complex transmission cycle involving freshwater, snails and human-water contact. Although Mass Drug Administration (MDA) with praziquantel remains the cornerstone of the control efforts, rapid reinfection often limits its long-term effectiveness. In this study, we develop a novel nonlinear compartmental model that couples human and snail dynamics while incorporating three time-dependent control measures: MDA, molluscicide for snail reduction, and water-contact reduction to reduce human-water contact. We apply Pontryagin's Maximum Principle to derive optimal strategies and simulate four intervention combinations. Our results reveal that while single or dual interventions moderately reduce transmission, the triple-intervention strategy most effectively suppresses both human and snail infections. Crucially, we extend the analysis by evaluating the cost-effectiveness of each strategy using metrics such as the IAR, ACER, and ICER. Findings indicate that the integrated approach not only maximizes health benefits but it is also economically justified, with some strategies demonstrating cost savings alongside epidemiological gains.

How to cite this article:

A. S. Afolabi and J. C. Orji., "MATHEMATICAL MODELLING AND OPTIMAL CONTROL ANALYSIS OF TRIPLE-INTERVENTION STRATEGIES FOR SCHISTOSOMIASIS MANAGEMENT IN ENDEMIC REGIONS", *BAREKENG: J. Math. & App.*, vol. 20, no. 4, pp. 3281-3304, Dec, 2026.

Journal homepage: *https://ojs3.unpatti.ac.id/index.php/barekeng/*
Journal e-mail: *barekeng.math@yahoo.com; barekeng.journal@mail.unpatti.ac.id*

Research Article · **Open Access**

1. INTRODUCTION

Schistosomiasis remains a major neglected tropical disease, especially in tropical and subtropical regions, and is often described as a "disease of poverty" [1], [2]. The World Health Organization (WHO) reports that roughly 250 million people are currently infected with the disease and about 700 million are living in endemic areas [2]. Over 90% of infections occur in sub-Saharan Africa [2], causing about 24,000 deaths and 2.5 million disability-adjusted life years (DALYs) each year [2]. The infection is acquired when people come in contact with freshwater containing schistosome larvae (cercariae) released by snail hosts. The infectious larvae breach the skin, access the bloodstream, and are carried to the liver for development into adults. The mature worms then travel to the blood vessels surrounding the intestines or bladder to mate and produce eggs. Some of these eggs exit the body through urine or feces, continuing the cycle when they reach water and hatch into miracidia that infect snails [1], [2]. Chronic infection causes serious morbidity-anemia, growth stunting, organ fibrosis, and in the case of S. haematobium urogenital disease including female genital schistosomiasis [3], [4]. Despite decades of mass praziquantel treatment campaigns [1], schistosomiasis remains endemic in many countries. This persistent burden, acknowledged in WHO's recent 2030 roadmap for schistosomiasis elimination underscores the need for integrated control strategies [1], [5].

Preventive chemotherapy (PC) with praziquantel is the cornerstone of current control. WHO guidelines recommend periodic mass drug administration (MDA) to groups at-risk to reduce heavy infections [3]. However, treatment coverage is often incomplete: in 2023 only about 56% of school-aged children in need actually received praziquantel [2], [6]. Even where MDA is delivered, reinfection is common in highly endemic areas. WHO and experts therefore emphasized that drug treatment alone was not enough. Complementary measures, notably snail control and improved water/sanitation (WASH) are needed to interrupt transmission [1], [3]. Snail-targeting interventions have historically proven effective at breaking transmission cycles [5], [4]. For example, intensive molluscicide efforts in places like Zanzibar and China dramatically reduced snail populations and disease prevalence [4], [5]. Likewise, provision of safe water and sanitation reduces people's exposure to infested water, preventing reinfection [1], [3]. In practice, many control programs now combine MDA with focal snail control and improvements in water/sanitation [1].

Classic models (building on Anderson-May frameworks) link human and snail populations to capture the parasite life cycle [7]. Numerous models have explored individual interventions, for example, the impacts of repeated MDA or reducing snail density and have incorporated factors like heterogeneous contact patterns, immunity, and spatial variation have been examined [7], [4]. Furthermore, [8] evaluated the long-term impact of MDA across varying transmission intensities and concluded that, although MDA significantly lowers prevalence, it is rarely sufficient to interrupt transmission on its own. Similarly, [9] extended this understanding by integrating ecological feedback mechanisms between snail and human populations, thereby illustrating how environmental seasonality can either reinforce or undermine control efforts. In contrast, [10] focused on chemical-based snail control and showed through meta-analysis that, when optimally timed and localized, molluscicide can substantially enhance the effectiveness of MDA. Moreover, [11] emphasized the need for spatial precision by introducing geographically explicit risk models, which revealed that uniform interventions may miss critical hotspots. Additionally, [12] underscored the influence of human mobility and seasonal water-contact patterns, arguing that such behavioural dynamics are often overlooked but can critically sustain transmission even under active intervention. However, despite these advances, most existing models focus on single or partially combined interventions and often do not simultaneously incorporate mass drug administration, snail control, and WASH strategies within a unified framework [13], [14], [15]. Furthermore, the integration of these interventions with optimal control approaches remains limited, restricting the ability to determine cost-effective and sustainable strategies for disease control.

In instances where public health resources are constrained, identifying effective interventions and allocating resources between competing strategies is critical. Optimal control theory offers a rigorous mathematical framework for solving such problems by allowing for the identification of time-dependent intervention strategies that minimize the burden of disease and take into account the cost of implementation. This study addresses the identified gaps through the development of a novel compartmental model that explicitly integrates mass drug administration, snail control, and WASH-based interventions within a single analytical framework. The model incorporates detailed human infection dynamics alongside snail population processes, allowing for a comprehensive representation of schistosomiasis transmission. Furthermore, the integration of these interventions into an optimal control framework distinguishes this work from previous studies. By applying Pontryagin's Maximum Principle, the study derives necessary conditions for determining optimal intervention strategies under resource constraints. Numerical simulations are then used

to evaluate the effectiveness and cost-efficiency of different control combinations. The findings provide important insights into how integrated strategies can be optimally deployed to reduce disease burden, thereby offering practical guidance for policymakers and contributing to ongoing efforts toward schistosomiasis control and elimination.

2. RESEARCH METHODS

We consider a deterministic compartmental model for the transmission dynamics of schistosomiasis, dividing both hosts and intermediate snail vectors into epidemiologically relevant classes. Let the total human population at time t be

$$N_h(t) = S_h(t) + E_h(t) + A_h(t) + I_h(t) + T_h(t), \tag{1}$$

where S_h denotes susceptible, E_h those exposed but not yet infectious, A_h asymptomatic carriers, I_h symptomatic infectious individuals, and T_h treated individuals. Likewise, the entire snail population is defined as

$$Ns(t) = S_s(t) + E_s(t) + I_s(t), \tag{2}$$

where S_s represents susceptible snails, E_s exposed snails in the pre-patent period, and I_s patent, cercariae-shedding snails.

The two free-living parasite stages in the aquatic environment mediate host-vector transmission: miracidia $N_m(t)$ and cercariae $N_c(t)$. Human recruitment (birth or immigration) occurs at constant rate Λ_h. Susceptible S_h are infected upon contact with cercariae at the saturating incidence rate

$$\lambda_h = \frac{\beta_h N_c}{c_0 + \epsilon N_c}, \tag{3}$$

where β_h is the maximum per-cercaria transmission rate, c_0 the half-saturation constant, and ϵ a crowding parameter whereas susceptible snails, S_s, acquire infection from miracidia at

$$\lambda_s = \frac{\beta_s N_m}{m_0 + \epsilon N_m}, \tag{4}$$

with parameters β_s, m_0 analogous to the human incidence.

This functional form in Eqs. (3) and (4) represents a saturating incidence rate, where the parameter ϵ accounts for crowding or interference effects that reduce transmission efficiency at high parasite densities [16], [17].

The flowchart for the proposed model population dynamics is given below:

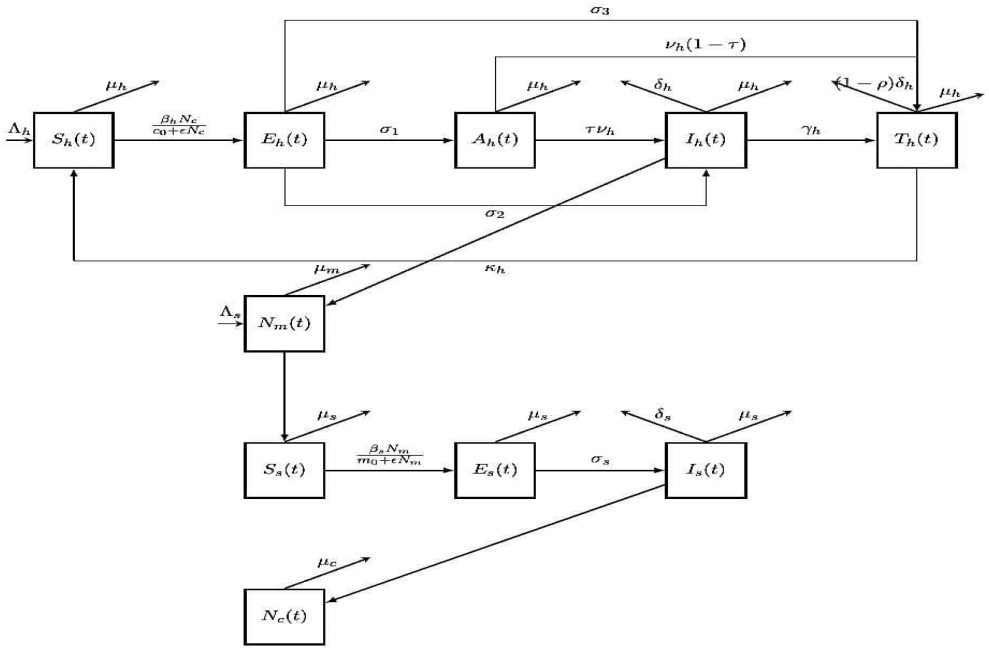

Figure 1. Schematic Diagram for the Model

The model structure is summarized schematically in Fig. 1, which shows the flow of humans and snails through susceptible, exposed, and infected states, as well as the environmental parasite compartments (N_m and N_c). Infected humans (I_h) release miracidia (N_m) into the environment, which in turn infect susceptible snails (S_s). Infected snails (I_s) release cercariae (N_c), completing the transmission cycle.

Accordingly, the described dynamics are governed by the subsequent system of non-linear ordinary differential equations (DE):

$$\begin{aligned}
\frac{dS_h}{dt} &= \Lambda_h + \kappa_h T_h - \frac{\beta_h N_c S_h}{c_0+\epsilon N_c} - \mu_h S_h,\\
\frac{dE_h}{dt} &= \frac{\beta_h N_c S_h}{c_0+\epsilon N_c} - \sigma_1 E_h - \sigma_2 E_h - \sigma_3 E_h - \mu_h E_h,\\
\frac{dA_h}{dt} &= \sigma_1 E_h - \nu_h A_h - \mu_h A_h,\\
\frac{dI_h}{dt} &= \sigma_2 E_h + \tau\nu_h A_h - \gamma_h I_h - (\delta_h + \mu_h) I_h,\\
\frac{dT_h}{dt} &= \sigma_3 E_h + \nu_h(1-\tau) A_h + \gamma_h I_h - \kappa_h T_h - \big((1-\rho)\delta_h + \mu_h\big) T_h,\\
\frac{dN_m}{dt} &= \lambda_m I_h - \mu_m N_m,\\
\frac{dS_s}{dt} &= \Lambda_s - \frac{\beta_s N_m S_s}{m_0+\epsilon N_m} - \mu_s S_s,\\
\frac{dE_s}{dt} &= \frac{\beta_s N_m S_s}{m_0+\epsilon N_m} - \sigma_s E_s - \mu_s E_s,\\
\frac{dI_s}{dt} &= \sigma_s E_s - \delta_s I_s - \mu_s I_s,\\
\frac{dN_c}{dt} &= \lambda_c I_s - \mu_c N_c.
\end{aligned} \tag{5}$$

with the initial conditions

$$S_h(0) > 0, E_h(0) \geq 0, A_h(0) \geq 0\,, I_h(0) > 0\,, T_h(0) \geq 0, N_m(0) > 0, S_s(0) \geq 0, E_s(0) \geq 0, I_s(0) > 0$$
$$and$$
$$N_c(0) > 0 \tag{6}$$

The model presented in this study is a modification of the schistosomiasis transmission framework developed by [18]. The primary difference between the original model and the present model is the introduction of an asymptomatic infected human compartment (A_h). In the original model, exposed individuals (E_h) progressed directly to chronic infection (I_h). In contrast, the present model incorporates an asymptomatic stage, allowing exposed individuals to first become asymptomatic carriers before progressing to chronic infection or recovering. This refinement provides a more realistic representation of schistosomiasis natural history, as many infected individuals remain asymptomatic for extended periods and may contribute to transmission without exhibiting clinical symptoms.

The model is formulated based on the following key assumptions:

1. The human and snail populations are replenished through constant recruitment rates $\Lambda_h$and Λ_s, respectively.
2. Infection is acquired only through contact with cercariae in contaminated water; there is no mother-to-child transmission.
3. Per-parasite transmission efficiency declines at high parasite densities due to crowding or spatial heterogeneity.
4. Asymptomatic individuals (A_h) can transmit infection and are the primary target of MDA.
5. Chronically infected individuals may recover and subsequently experience relapse, reflecting reinfection or treatment failure.
6. Infected snails do not recover or receive treatment; they remain infected until death.

RESULTS AND DISCUSSION

3.1 Qualitative Analysis of the Model

The qualitative analysis of the model examines its theoretical behavior by assessing key properties such as positivity, boundedness, and equilibrium states.

3.1.1 Analysis of Solution Positivity and Boundedness

Theorem 1. *The positive orthant is invariant under system (5); solutions initiating with positive values remain positive for all.* $t > 0, S_h(0), E_h(0), A_h(0), I_h(0), T_h(0), N_m(0), E_s(0), I_s(0)$ *and* $N_c(0) > 0$.

Proof. Let $t_1 = \sup\{t > 0: S_h(0) > 0, E_h(0) \geq 0, A_h(0) \geq 0, I_h(0) > 0, T_h(0) \geq 0, N_m(0) > 0, S_s(0) \geq 0, E_s(0) \geq 0, I_s(0) > 0, N_c(0) > 0 \in [0, t]\}$. Hence, the first equation of the schistosomiasis Eq. (5) is written as

$$\frac{dS_h}{dt} = \Lambda_h + \kappa_h T_h - \lambda_h S_h - \mu_h S_h \geq \Lambda_h - \lambda_h S_h - \mu_h S_h \tag{7}$$

where $\lambda_h = \frac{\beta_h N_c}{c_0 + \epsilon N_c}$. Therefore,

$$S_h(t_1) \quad \geq S_h(0) e^{\left(-\mu_h t - \int_0^t \lambda_h dt\right)} + e^{\left(-\mu_h t - \int_0^t \lambda_h dt\right)} \times \Lambda_h \int_0^{t_1} e^{\left(\mu_h t + \int_0^t \lambda_h(\psi) d\psi\right)} dt \geq 0$$

In the same way, it can be shown that $E_h \geq 0, A_h \geq 0, I_h \geq 0, T_h \geq 0, N_m \geq 0, E_s \geq 0, I_s \geq 0$ and $N_c \geq 0$.

By analysing the system within its biologically relevant phase space, comprising $\Omega = \Omega_h \cup \Omega_v \subset \mathcal{R}_+^5 \times \mathcal{R}_+^3$ with

$$\Omega_h = \left\{(S_h, E_h, A_h, I_h, T_h) \in \mathcal{R}_+^5 : S_h + E_h + A_h + I_h + T_h = N_h \leq \frac{\Lambda_h}{\mu_h}\right\} \text{ and}$$

$$\Omega_s = \left\{(S_s, E_s, I_s) \in \mathcal{R}_+^3 : S_s + E_s + I_s = N_s \leq \frac{\Lambda_s}{\mu_s}\right\}.$$

Theorem 2. *The region* $\Omega = \Omega_h \cup \Omega_s \subset \mathcal{R}_+^5 \times \mathcal{R}_+^3$ *remains a positively invariant region for schistosomiasis model in Eq. (5) given any non-negative initial condition in* $\mathcal{R}_+^8$.

Proof. An analysis of Eq. (5) reveals that

$$\frac{dN_h(t)}{dt} = \frac{dS_h}{dt} + \frac{dE_h}{dt} + \frac{dA_h}{dt} + \frac{dI_h}{dt} + \frac{dT_h}{dt}, \tag{8}$$

Similarly,

$$\frac{dN_s(t)}{dt} = \frac{dS_s}{dt} + \frac{dE_s}{dt} + \frac{dI_s}{dt}. \tag{9}$$

Eqs. (8) and (9) yields:

$$N_h(t) \leq N_h(0) e^{-\mu_h t} + \frac{\Lambda_h}{\mu_h}(1 - e^{-\mu_h t}),$$

and

$$N_s(t) = N_s(0) e^{-\mu_s t} + \frac{\Lambda_s}{\mu_s}(1 - e^{-\mu_s t}). \tag{10}$$

Thus, $N_h(t) \leq N_h(0) e^{-\mu_h t} + \frac{\Lambda_h}{\mu_h}(1 - e^{-\mu_h t})$ and $N_s(t) = N_s(0) e^{-\mu_s t} + \frac{\Lambda_s}{\mu_s}(1 - e^{-\mu_s t})$. Specifically, $N_h(t) \leq \frac{\Lambda_h}{\mu_h}$ and $N_s(t) = \frac{\Lambda_s}{\mu_s}$, given that $N_h(0) \leq \frac{\Lambda_h}{\mu_h}$ and $N_s(0) \leq \frac{\Lambda_s}{\mu_s}$. Consequently, the region remains positively-invariant. Furthermore, if $N_h(t) > \frac{\Lambda_h}{\mu_h}$ and $N_s(t) > \frac{\Lambda_s}{\mu_s}$, then the trajectories will either enter the region Ω within a finite time or, asymptotically, $N_h(t)$ and $N_s(t)$ will converge to $\frac{\Lambda_h}{\mu_h}$ and $\frac{\Lambda_s}{\mu_s}$ respectively.

3.1.2 Existence and Stability of the Disease-Free Equilibrium (DFE)

The DFE, a critical state within the schistosomiasis transmission model, corresponds to the absence of infection, characterized by zero infected populations (i.e., $I_h = 0$ and $I_s(t) = 0$). Equating the LHS of model to zero and computing the simultaneous solution of the resultant equations yields the model's equilibrium solutions. The specific solution representing the disease-free state is given by:

$$\begin{aligned}\mathcal{E}_0 &= (S_h^*, E_h^*, A_h^*, I_h^*, T_h^*, S_s^*, E_s^*, I_s^*)\\ &= \left(\frac{\Lambda_h}{\mu_h}, 0,0,0,0, \frac{\Lambda_s}{\mu_s}, 0,0\right)\end{aligned} \tag{11}$$

The DFE is evaluated for stability using the basic reproduction number, following the approach and notation outlined in [18], [19] for matrix F (new infections) and matrix V (transition terms). It follows that the leading eigenvalue of the next-generation matrix, of (FV^{-1}) for Eq. (5), yields

$$F = \begin{pmatrix} 0 & 0 & 0 & 0 & 0 & 0 & 0 & \frac{\beta_h S_h}{\epsilon N_c + c_0} - \frac{\beta_h N_c S_h \epsilon}{(\epsilon N_c + c_0)^2} \\ 0 & 0 & 0 & 0 & 0 & 0 & 0 & 0 \\ 0 & 0 & 0 & 0 & 0 & 0 & 0 & 0 \\ 0 & 0 & 0 & 0 & 0 & 0 & 0 & 0 \\ 0 & 0 & 0 & 0 & 0 & 0 & 0 & 0 \\ 0 & 0 & 0 & 0 & \frac{\beta_s S_s}{\epsilon N_m + m_0} - \frac{\beta_s N_m S_s \epsilon}{(\epsilon N_m + m_0)^2} & 0 & 0 & 0 \\ 0 & 0 & 0 & 0 & 0 & 0 & 0 & 0 \\ 0 & 0 & 0 & 0 & 0 & 0 & 0 & 0 \end{pmatrix}$$

$$V = \begin{pmatrix} \sigma_1 + \sigma_2 + \sigma_3 + \mu_h & 0 & 0 & 0 & 0 & 0 & 0 & 0 \\ -\sigma_1 & \mu_h + \nu_h & 0 & 0 & 0 & 0 & 0 & 0 \\ -\sigma_2 & -\tau\,\nu_h & \gamma_h + \delta_h + \mu_h & 0 & 0 & 0 & 0 & 0 \\ -\sigma_3 & -\nu_h(1-\tau) & -\gamma_h & \kappa_h + (1-\rho)\delta_h + \mu_h & 0 & 0 & 0 & 0 \\ 0 & 0 & -\lambda_m & 0 & \mu_m & 0 & 0 & 0 \\ 0 & 0 & 0 & 0 & 0 & \mu_s + \sigma_s & 0 & 0 \\ 0 & 0 & 0 & 0 & 0 & -\sigma_s & \delta_s + \mu_s & 0 \\ 0 & 0 & 0 & 0 & 0 & 0 & -\lambda_c & \mu_c \end{pmatrix}$$

$$R_0 = \sqrt{\frac{\beta_s \Lambda_s \beta_h \Lambda_h \sigma_s (\mu_h \sigma_2 + \nu_h(\tau\,\sigma_1 + \sigma_2))\lambda_m \lambda_c}{(\delta_s+\mu_s)(\mu_h+\nu_h)(\gamma_h+\delta_h+\mu_h)\mu_m \mu_c (\mu_s+\sigma_s)(\sigma_1+\sigma_2+\sigma_3+\mu_h) m_0 c_0 \mu_h \mu_s}} \tag{12}$$

Theorem 3. *For system (5), the DFE. $\mathcal{E}_0$, given in Equation (11) is locally asymptotically stable (LAS) when $R_0 < 1$, and unstable when $R_0 > 1$.*

Proof. To prove Theorem 3, the Jacobian matrix of Eq. (5) must be linearized at $\mathcal{E}_0$

$$J = \begin{pmatrix} 0 & 0 & 0 & 0 & 0 & 0 & 0 & 0 & 0 & -\frac{S_h \beta_h}{\epsilon N_c + c_0} + \frac{S_h \beta_h N_c \epsilon}{(\epsilon N_c + c_0)^2} \\ 0 & 0 & 0 & 0 & 0 & 0 & 0 & 0 & 0 & \frac{S_h \beta_h}{\epsilon N_c + c_0} - \frac{S_h \beta_h N_c \epsilon}{(\epsilon N_c + c_0)^2} \\ 0 & 0 & 0 & 0 & 0 & 0 & 0 & 0 & 0 & 0 \\ 0 & 0 & 0 & -\gamma_h - \delta_h - \mu_h & 0 & 0 & 0 & 0 & 0 & 0 \\ 0 & 0 & 0 & \gamma_h & 0 & 0 & 0 & 0 & 0 & 0 \\ 0 & 0 & 0 & \lambda_m & 0 & -\mu_m & 0 & 0 & 0 & 0 \\ 0 & 0 & 0 & 0 & 0 & -\frac{\beta_s S_s}{\epsilon N_m + m_0} + \frac{\beta_s N_m S_s \epsilon}{(\epsilon N_m + m_0)^2} & -\frac{\beta_s N_m}{\epsilon N_m + m_0} - \mu_s & 0 & 0 & 0 \\ 0 & 0 & 0 & 0 & 0 & \frac{\beta_s S_s}{\epsilon N_m + m_0} - \frac{\beta_s N_m S_s \epsilon}{(\epsilon N_m + m_0)^2} & \frac{\beta_s N_m}{\epsilon N_m + m_0} - \mu_s & -\sigma_s & 0 & 0 \\ 0 & 0 & 0 & 0 & 0 & 0 & 0 & \sigma_s & -\delta_s - \mu_s & 0 \\ 0 & 0 & 0 & 0 & 0 & 0 & 0 & 0 & \lambda_c & -\mu_c \end{pmatrix} \tag{13}$$

The characteristic polynomial, $P(\lambda^*)$ of Eq. (13) is given as

$$P(\lambda^*) = |J(\mathcal{E}_0) - \lambda^* \mathbb{I}_8| \tag{14}$$

$$P(\lambda^*) = \lambda^4(\lambda + \sigma_s)(\lambda + \mu_s)(\lambda + \mu_s + \delta_s)(\lambda + \mu_m)(\lambda + \mu_h + \delta_h + \gamma_h)(\lambda + \mu_c) \tag{15}$$

The eigenvalues of Eq. (15) are given as

$$\lambda_i^* = (-\mu_c, -\mu_s, -\mu_s - \delta_s, -\sigma_s, -\mu_m, 0, 0, 0, 0, -(\gamma_h + \mu_h + \delta_h))^T \tag{16}$$

The presence of zero eigenvalues (multiplicity 4) indicates that $\mathcal{E}_0$ is non-hyperbolic. Therefore, linearization alone is insufficient to determine stability when $R_0 = 1$. We must apply the Centre Manifold Theorem to analyse the behaviour on the centre manifold.

Let ϕ be a bifurcation parameter chosen such that $R_0 = 1$ when $\phi = 0$. Following the approach of [19], we analyze the system near $\mathcal{E}_0$ at $\phi = 0$.

Let $x = (x_1, x_2, \dots, x_{10})^T$ be the vector of state variables with $\mathcal{E}_0$ at the origin. We rewrite Eq. (5) as $\frac{dx}{dt} = f(x, \phi)$, where $f(0, \phi) = 0$ for all ϕ. The Jacobian $J = D_x f(0,0)$ has a simple zero eigenvalue with right eigenvector w and left eigenvector v satisfying:

$$Jw = 0, J^T v = 0, v \cdot w = 1.$$

The dynamics on the centre manifold are governed by:

$$\frac{du}{dt} = \frac{a}{2}u^2 + bu\phi + \text{higher-order terms}$$

where the coefficients a and b are given by:

$$a = \sum_{k,i,j=1}^{10} v_k\, w_i w_j \frac{\partial^2 f_k}{\partial x_i\, \partial x_j}(0,0),\ b = \sum_{k,i=1}^{10} v_k\, w_i \frac{\partial^2 f_k}{\partial x_i\, \partial \phi}(0,0)$$

After computing the eigenvectors and second-order partial derivatives, we obtain, $b = \frac{\partial R_0}{\partial \phi} > 0 \cdot$

$$a = -\frac{2\mu_c}{\sigma_1 + \sigma_2 + \sigma_3 + \mu_h} \cdot \frac{\beta_s \Lambda_s \beta_h \Lambda_h \sigma_s \lambda_m \lambda_c}{(\delta_s + \mu_s)(\nu_h + \mu_h)(\gamma_h + \delta_h + \mu_h)\mu_m(\mu_s + \sigma_s)m_0 c_0 \mu_h \mu_s} \cdot \frac{\sigma_1}{\sigma_1 + \sigma_2 + \sigma_3 + \mu_h} < 0$$

Since $a < 0$ and $b > 0$, the system undergoes a transcritical bifurcation at $R_0 = 1$. The bifurcation is forward (supercritical), meaning: For $R_0 < 1$ (i.e., $\phi < 0$), the only equilibrium is the DFE, which is locally asymptotically stable. For $R_0 > 1$ (i.e., $\phi > 0$), the DFE becomes unstable, and a stable endemic equilibrium emerges. Therefore, the disease-free equilibrium $\mathcal{E}_0$ is locally asymptotically stable when $R_0 < 1$, and unstable when $R_0 > 1$.

3.2 Estimation of Model Parameters and Initial Conditions

The estimation of model parameters and initial conditions involves determining the numerical values that best describe the schistosomiasis model's dynamics, ensuring that the model accurately reflects real-world data and initial population states.

3.2.1 Estimation of Initial Conditions

In calibrating the initial conditions for our schistosomiasis transmission model, we adopt field-informed assumptions rooted in observed prevalence data from endemic settings. Assuming a total human population of $N_h(0) = 10{,}000$, and a schistosomiasis prevalence of $P_h = 0.20$ (i.e., 20%), we infer an initial infected human population of $I_h(0) = P_h \times N_h(0) = 2000$ individuals. Empirical data suggest that 60% of infected individuals are asymptomatic while the remaining 40% are symptomatic [20]. This yields $A_h(0) = 0.60 \times I_h(0) = 1200$ asymptomatic individuals and $I_h(0) = 0.40 \times \text{Total Infected} = 800$ symptomatic individuals. If MDA coverage reached 40% of infected individuals, then we estimate $T_h(0) = 0.40 \times I_h(0) = 800$ treated individuals. Assuming no individuals are in the exposed class at $t = 0$, we set $E_h(0) = 0$. Therefore,

$$S_h(0) = N_h(0) - \big(A_h(0) + I_h(0) + T_h(0)\big) = 10{,}000 - (1200 + 800 + 800) = 7200.$$

For the snail intermediate host, we assume an initial population of $N_s(0) = 5000$ with a patent infection prevalence of $P_s = 0.03$ (3%) [21]. This results in $I_s(0) = P_s \times N_s(0) = 150$ infected snails. Assuming negligible pre-patent infection, we set $E_s(0) = 0$, and consequently $S_s(0) = N_s(0) - I_s(0) = 4850$ susceptible snails.

Environmental stages are highly ephemeral due to high mortality rates of miracidia and cercariae. Assuming daily per capita mortality rates of $\mu_m = 2.4$ and $\mu_c = 1.7$ respectively, and production rates $\lambda_m = 500\ \text{d}^{-1}$ and $\lambda_c = 900\ \text{d}^{-1}$ [22], we estimate the equilibrium densities of free-living stages as:

$$N_m(0) = \frac{\lambda_m I_h(0)}{\mu_m} = \frac{500 \times 800}{2.4} \approx 166{,}667, \quad N_c(0) = \frac{\lambda_c I_s(0)}{\mu_c} = \frac{900 \times 150}{1.7} \approx 79{,}412.$$

3.2.2 Estimation of Parameters

In developing a biologically plausible model of schistosomiasis transmission dynamics, careful estimation of each parameter is essential to ensure realism and validity. The human recruitment rate Λ_h is chosen so that, in the absence of infection, births balance deaths at the prevailing population size. For an adult life expectancy of roughly 60 years in Nigeria [23] ($\mu_h = 4.6 \times 10^{-5}\ \text{d}^{-1}$) and a baseline population $N_h^0 = 10\,000$, we set

$$\Lambda_h = \mu_h N_h^0 \approx (4.6 \times 10^{-5}\ \text{d}^{-1})(10\,000) = 0.46\ \text{individuals d}^{-1},$$

ensuring demographic equilibrium in the disease-free state [24]. Similarly, snails (e.g. *Biomphalaria* spp.) are highly fecund and often outnumber humans; with a natural mortality $\mu_s \approx 0.01\ \mathrm{d}^{-1}$ (average lifespan $\sim$ 100 d) and $N_s^0 = 5000$ in the focal habitat, we take

$$\Lambda_s = \mu_s N_s^0 \approx (0.01\ \mathrm{d}^{-1})(5\,000) = 50\ \text{snails}\ \mathrm{d}^{-1},$$

maintaining a stable snail population in the absence of infection [21]. The human natural mortality rate, μ_h, is typically based on the average life expectancy; for a lifespan of approximately 60 years, μ_h is estimated as $\frac{1}{60yr} \approx \frac{1}{60\times365d} \approx 4.6 \times 10^{-5}\ \mathrm{d}^{-1}$ [24]. For snails, specifically *Biomphalaria* species, the natural death rate, μ_s, varies with environmental conditions, ranging from 0.001 to 0.022 d^{-1}, with a central estimate of 0.01 d^{-1} representing moderate conditions [21]. Miracidia and cercariae, the free-living larval stages of the parasite, have short lifespans, with miracidia surviving on average 10 hours (0.417 d) and cercariae about 14 hours (0.583 d) in freshwater; this translates to decay rates of approximately $\mu_m \approx \frac{1}{0.417} \approx 2.4\ \mathrm{d}^{-1}$ and $\mu_c \approx \frac{1}{0.583} \approx 1.7\ \mathrm{d}^{-1}$ respectively [22], [25].

Regarding progression rates within the human host, the average latent (prepatent) period before schistosome egg shedding is observed ranges between 25 to 30 days. This suggests a combined progression rate from exposure to infectiousness of $\sigma_1 + \sigma_2 + \sigma_3 + \mu_h \approx 0.036\ \mathrm{d}^{-1}$ [26], [27]. Infected snails also exhibit a latent period (prepatency) of about 18 to 45 days, yielding a central estimate of $\sigma_s \approx \frac{1}{31.5} \approx 0.032\ \mathrm{d}^{-1}$ [7], [28]. Treatment rates depend on health-seeking behavior and detection strategies; asymptomatic individuals may only be treated during routine screenings, approximated as once every 180 days, giving $\nu_h \approx \frac{1}{180} \approx 0.0056\ \mathrm{d}^{-1}$, while symptomatic individuals may seek treatment within two weeks, yielding $\gamma_h \approx \frac{1}{14} \approx 0.071\ \mathrm{d}^{-1}$ [29], [30].

Parasite shedding rates are also critical to transmission. An infected human with a light to moderate worm burden may produce approximately 7,000 eggs per week, with roughly 50% hatching into miracidia, leading to an estimate of $\lambda_m \approx 500$ miracidia per day [7], [31]. Infected snails can shed 6,000-6,800 cercariae weekly, suggesting a daily output of about 900 cercariae (λ_c) [31], [32]. Transmission rates from parasite stages to hosts are captured by coefficients β_h and β_s, representing the rate at which cercariae infect humans and miracidia infect snails, respectively. These rates, typically ranging from 10^{-4} to 10^{-2} per parasite per day, are incorporated into a Holling type II functional response to capture saturation effects at high parasite densities [33]. The half-saturation constants c_0 and m_0 are assumed to be on the order of 10^4 cercariae or miracidia, representing the environmental density at which the transmission rate reaches half its maximum. The saturation scaling factor ϵ is often set between 1 and 10 to fine-tune the curvature of the response function [34].

Table 1. Parameter Descriptions for the Schistosomiasis Transmission Model

Parameter	Description	Value	Source
Λ_h	Recruitment rate of humans	0.46 d^{-1}	Estimate
κ_h	Rate at which treated humans lose prophylactic protection and return to the susceptible pool	0.0056 d^{-1}	Estimate
β_h	Maximum transmission rate from cercariae to humans	10^{-3} d^{-1}	Estimate
c_0	Half-saturation constant in the human incidence function	10^4 parasites	Estimate
ϵ	Crowding/scaling parameter in both human and snail incidence functions	0.2	[12]
μ_h	Natural mortality rate of humans	4.6×10^{-5} d^{-1}	Estimate
σ_1	Rate at which exposed humans become asymptomatic carriers	0.25 d^{-1}	Estimate
σ_2	Rate at which exposed humans become infectious	0.008 d^{-1}	Estimate
σ_3	Rate at which exposed humans are treated directly	0.003 d^{-1}	Estimate
ν_h	Treatment rate of asymptomatic humans	0.0056 d^{-1}	Estimate
T	Proportion of treated asymptomatic individuals who do not fully recover and progress to symptomatic infection	0.1	Estimate
γ_h	Treatment rate of infectious humans	0.071 d^{-1}	Estimate
Δ_h	Disease-induced mortality rate in symptomatic humans	0.0014 d^{-1}	Assumed
Λ_m	Production rate of free-living miracidia per infected human	500 miracidia·d^{-1}	Estimate
μ_m	Natural mortality rate of miracidia	2.4 d^{-1}	Assumed
Λ_s	Recruitment rate of snails	50 d^{-1}	Estimate
β_s	Maximum transmission rate from miracidia to snails	10^{-3} d^{-1}	Estimate
m_0	Half-saturation constant in the snail incidence function	10^{-4} parasites	Estimate

Parameter	Description	Value	Source
μ_s	Natural mortality rate of snails	0.01 d^{-1}	Estimate
σ_s	Rate at which exposed snails become infectious	0.032 d^{-1}	Estimate
δ_s	Disease-induced mortality rate in infected snails	0.0004012 d^{-1}	[12]
λ_c	Production rate of free-living cercariae per infected snail	900 cercariae·d^{-1}	Estimate
μ_c	Natural mortality rate of cercariae	1.7 d^{-1}	Assumed

3.3 Sensitivity Analysis

The normalized forward sensitivity index (SI) of R_0, with respect to a differentiable parameter Z, is defined by the expression [35], [36]

$$S_Z^{R_0} = \frac{\partial R_0}{\partial Z} \times \frac{Z}{R_0} \tag{17}$$

As an illustration, the sensitivity measure of R_0 for Eq. (5) with reference to the parameter β_h, is provided by the following expression:

$$S_{\beta_h}^{R_0} = \frac{\partial R_0}{\partial \beta_h} \times \frac{\beta_h}{R_0} = \frac{1}{2} \tag{18}$$

Applying the method to the remaining parameters, the SI of each parameter of R_0 is listed in Table 2 below:

Table 2. Sensitivity Indices

Parameter	SI	Parameter	SI	Parameter	SI
T	0.01503	δ_s	-0.19286	μ_m	-0.5
Λ_h	0.5	γ_h	-0.49869	μ_s	-1.0
Λ_s	0.5	λ_c	0.5	ν_h	0.00012
c_0	-0.5	Λ_m	0.5	σ_1	-0.331747
β_h	0.5	m_0	-0.5	σ_2	0.373999
β_s	0.5	μ_c	-0.5	σ_3	-0.41613
δ_h	-0.000983	μ_h	-0.50108	σ_s	0.11905

From Table 2, the most influential parameters can be ranked according to the magnitude of their sensitivity indices. The human recruitment rate (Λ_h), snail recruitment rate (Λ_s), and transmission rates (β_h, β_s) exhibit the highest positive sensitivity values, indicating that increases in these parameters significantly enhance disease transmission. Similarly, the environmental shedding rates (λ_c, λ_m) also contribute positively to R_0, though with slightly lower magnitudes. On the other hand, the snail natural death rate (μ_s) has the largest negative SI, making it the most influential parameter in reducing R_0. This is followed by the human recovery rate $(\gamma_h)$and the death rates of cercariae and miracidia (μ_c, μ_m), which also exhibit substantial negative sensitivities. These results suggest that increasing snail mortality, improving treatment outcomes, and reducing parasite survival in the environment are effective strategies for disease control. Furthermore, the parameter σ_2, representing the progression rate from exposed to infectious individuals, shows a positive SI, reflecting its role in increasing the number of infectious individuals. In contrast, σ_3, which represents treatment of exposed individuals, has a strong negative SI, highlighting the importance of early diagnosis and intervention. Overall, the sensitivity analysis emphasizes that vector control (increasing μ_s), reducing transmission (β_h, β_s), improving treatment (γ_h, σ_3), and environmental management (μ_c, μ_m) are critical components for effective schistosomiasis control.

3.4 Analysis of Optimal Control

In the context of schistosomiasis epidemiology, the aim is to minimize human and snail infection burdens while accounting for the costs and logistical constraints of deploying control measures. By formulating an objective functional that balances infection prevalence against the economic and operational costs of these strategies, we seek to identify the optimal time-profiles of $u_1(t)$, $u_2(t)$, and $u_3(t)$ that achieve the greatest reduction in schistosomiasis cases and environmental contamination over the planning horizon.

3.4.1 The Proposed Control Measures

Mass Drug Administration (MDA) (u_1):

In the model, MDA directly increases the treatment rates of exposed (σ_3), asymptomatic (ν_h), and symptomatic (γ_h) individuals, thereby moving them into the treated class T_h. Treating exposed individuals (E_h) is included because praziquantel has efficacy against juvenile worms, and early treatment can prevent

progression to infectiousness and reduce transmission. This is particularly relevant for community-wide MDA programs where individuals may be treated before symptoms develop.

Snail Control via Molluscicide or Habitat Modification (u_2):

Interrupting the parasite's life cycle requires targeting its intermediate host. In the model, snail control adds directly to the natural mortality rate of susceptible, exposed, and infected snails' so that μ_s becomes $\mu_s + u_2(t)$.

Water Contact Reduction / Health Education (u_3):

Limiting human exposure to cercariae is another critical intervention. In the model's saturating incidence term, this control scales down the transmission coefficient from β_h to $\beta_h\left(1-u_3(t)\right)$.

$$\begin{cases} \frac{dS_h}{dt} = \Lambda_h + \kappa_h T_h - \frac{\beta_h (1-u_3) N_c S_h}{c_0+\epsilon N_c} - \mu_h S_h, \\ \frac{dE_h}{dt} = \frac{\beta_h (1-u_3) N_c S_h}{c_0+\epsilon N_c} - (\sigma_1 + \sigma_2 + \sigma_3 + u_1 + \mu_h)E_h, \\ \frac{dA_h}{dt} = \sigma_1 E_h - (\nu_h + u_1 + \mu_h)A_h, \\ \frac{dI_h}{dt} = \sigma_2 E_h + \tau(\nu_h + u_1)A_h - (\gamma_h + u_1 + \delta_h + \mu_h)I_h, \\ \frac{dT_h}{dt} = \sigma_3 E_h + (\nu_h + u_1)(1-\tau)A_h + (\gamma_h + u_1)I_h - \kappa_h T_h - \left((1-\rho)\delta_h + \mu_h\right)T_h, \\ \frac{dN_m}{dt} = \lambda_m I_h - \mu_m N_m, \\ \frac{dS_s}{dt} = \Lambda_s - \frac{\beta_s N_m S_s}{m_0+\epsilon N_m} - (\mu_s + u_2)S_s, \\ \frac{dE_s}{dt} = \frac{\beta_s N_m S_s}{m_0+\epsilon N_m} - (\sigma_s + \mu_s + u_2)E_s, \\ \frac{dI_s}{dt} = \sigma_s E_s - (\delta_s + \mu_s + u_2)I_s, \\ \frac{dN_c}{dt} = \lambda_c I_s - \mu_c N_c. \end{cases} \tag{19}$$

with the initial conditions given by Eq. (6). To achieve the desired goal, we define an objective functional that balances the cost of interventions against the burden of the disease. This functional takes the following form:

$$J(u_1,u_2,u_3) = Min \int_0^T \left[B_1 A_h(t) + B_2 I_h(t) + B_3 I_s(t) + \frac{W_1}{2} u_1(t)^2 + \frac{W_2}{2} u_2(t)^2 + \frac{W_3}{2} u_3(t)^2\right] dt, \tag{20}$$

B_1, B_2 and B_3 are weight constants that balance the cost of interventions against the importance of reducing infected populations A_h, I_h and I_s, while W_1, W_2, W_3, are positive weight constants that quantify the relative cost pertaining to the implementation of the control measures u_1, u_2 and u_3 over the fixed intervention period $[0, T]$. The use of quadratic terms to quantify the cost of the control measures is well-established in OC theory for epidemics, as demonstrated in prior research by [37], [38], [39]. The objective is to determine an OC triple $u_1^*, u_2^*,$ and u_3^* such that

$$J(u_1^*, u_2^*, u_3^*) = \min\{(u_1,u_2,u_3): u_1,u_2,u_3 \in \Omega\}, \tag{21}$$

where, $\Omega = \{u_i: 0 \le u_i(t) \le 1,$ is a Lebesgue measurable function, $t = [0,T]$ for $i = 1,2,3\}$ is the control set.

The application of OC in Eq. (19) allows for the investigation of the presence of OC while ensuring alignment with Pontryagin's Maximum Principle. Following the methodology in [40], we apply Pontryagin's principle to transform the problem into minimizing the point-wise Lagrangian, L, with respect to the controls u_1, u_2, u_3. This is achieved by analyzing the Hamiltonian, $(\mathcal{H})$, which reformulates Eqs. (19), (20), and (21) into a minimization problem.

$$\mathcal{H} = B_1 A_h + B_2 I_h + B_3 I_s + \frac{W_1}{2} u_1^2 + \frac{W_2}{2} u_2^2 + \frac{W_3}{2} u_3^2 + \lambda_{S_h}\left[\Lambda_h + \kappa_h T_h - \frac{\beta_h(1-u_3)N_c S_h}{c_0+\epsilon N_c} - \mu_h S_h\right] + \lambda_{E_h}\left[\frac{\beta_h(1-u_3)N_c S_h}{c_0+\epsilon N_c} - (\sigma_1+\sigma_2+\sigma_3+u_1+\mu_h)E_h\right] + \lambda_{A_h}[\sigma_1 E_h - (\nu_h+u_1+\mu_h)A_h] + \lambda_{I_h}[\sigma_2 E_h + \tau(\nu_h+u_1)A_h - (\gamma_h+u_1+\delta_h+\mu_h)I_h] + \lambda_{T_h}[\sigma_3 E_h + (\nu_h+u_1)(1-\tau)A_h + (\gamma_h +$$

$$u_1)I_h - \kappa_h T_h - \left((1-\rho)\delta_h + \mu_h\right)T_h] + \lambda_{N_m}[\lambda_m I_h - \mu_m N_m] + \lambda_{S_s}\left[\Lambda_s - \frac{\beta_s N_m S_s}{m_0+\epsilon N_m} - (\mu_s + u_2)S_s\right] + \lambda_{E_s}\left[\frac{\beta_s N_m S_s}{m_0+\epsilon N_m} - (\sigma_s + \mu_s + u_2)E_s\right] + \lambda_{I_s}[\sigma_s E_s - (\delta_s + \mu_s + u_2)I_s] + \lambda_{N_c}[\lambda_c I_s - \mu_c N_c]. \quad (22)$$

The necessary conditions for an optimal control problem include the adjoint system, optimality conditions, and projection formula. These are derived by applying Pontryagin's Maximum Principle, which yields a set of adjoint equations that govern the costate variables, as well as algebraic expressions for the optimal controls in terms of the state and costate variables. The full derivation of the adjoint system, optimality conditions, and projection formula is presented in the following section 3.4.2.

3.4.2 Existence of an Optimal Control

The existence of an OC for Eq. (20) with respect to the dynamics in Eq. (19) will be examined by applying the following theorems as outlined in [41], [35]. The results establish a rigorous framework for analyzing the system and defining the necessary conditions for achieving an OC strategy.

Theorem 4. *There exists* OC *triple* $u_i^* \in \Omega$ *for* $i = 1,2,3$ *that minimizes the objective functional* $J(u_1^*, u_2^*, u_3^*)$ *subject to the control Eq. (19) and its initial conditions in Eq. (6).*

Proof. To prove Theorem 4**.** We establish the following properties:

1. The control set Ω associated with each state variable equation is non-empty.
2. The control set is closed
3. The control set is convex
4. Nonnegative solutions of Eq. (19) exist and are bounded.
5. The boundedness of each right-hand side expression in Eq. (5) is a linear function of Ω, which varies with time and depends on the state variables.
6. The integrand in the objective function in Eq. (20), expressed as

$$B_1 A_h + B_2 I_h(t) + B_3 I_s(t) + \frac{1}{2}(W_1 u_1^2(t) + W_2 u_2^2(t) + W_3 u_3^2(t))$$

is convex in Ω

1. The control set Ω associated with each state variable equation is non-empty. This condition holds since all state and control variables within the set are non-negative and non-empty. Additionally, it is evident that the control function is Lebesgue integrable on [0, T].

2. A set is closed if it contains all its limit points, meaning that if a sequence of points in the set converges, then the limit of the sequence is also in the set.
   Consider the control set Ω given by $0 \le u_i(t) \le 1$ for $i = 1,2,3$ and all $t \in [0,T]$.

   The control set Ω is the set of all bounded measurable functions $u_i(t)$ such that $0 \le u_i(t) \le 1$. To show this set is closed, consider a sequence $\{u_i^n(t)\}$ in Ω that converges to a function $u_i(t)$ almost everywhere. For each n,

   $$0 \le u_i^n(t) \le 1$$

   It implies that if a series of constrained functions converge almost everywhere, their limit is likewise bounded by the same bounds:

   $$0 \le u_i(t) \le 1$$

   Hence, the limit $u_i(t)$ also lies within Ω, proving that Ω is closed.

3. A set is convex if, for any two points in the set, the line segment connecting them lies entirely within the set.
   In order to show convexity, consider any two functions $u_i^1(t)$ and $u_i^2(t)$ in Ω. For any $\alpha \in [0,1]$, define a convex combination of these two functions:

   $$u_i^\alpha(t) = \alpha u_i^1(t) + (1-\alpha)u_i^2(t)$$

   We need to show that $u_i^\alpha(t)$ also lies within Ω, i.e., $0 \le u_i^\alpha(t) \le 1$.

   Since $0 \le u_i^1(t) \le 1$ and $0 \le u_i^2(t) \le 1$,

   $$0 \le \alpha u_i^1(t) \le \alpha$$

and

$$0 \leq (1-\alpha)u_i^2(t) \leq (1-\alpha)$$

Adding these inequalities, we get:

$$0 \leq \alpha u_i^1(t) + (1-\alpha)u_i^2(t) \leq \alpha + (1-\alpha) = 1$$

Thus, $u_i^{\alpha}(t) \in \Omega$, proving that Ω is convex.

4. Given that the state and control variables in Eq. (19) are positive, and that the control set Ω is closed and convex as seen above, we consider the objective function $J(u_1, u_2, u_3)$. Since the integrand of J is a convex function of the control variables (u_1, u_2, u_3) on the control set Ω, the convexity implies that any local minimum is also a global minimum, which simplifies finding the optimal control.
Furthermore, there exist positive constants η_1, η_2, and $\epsilon > 1$ such that for any admissible control $\mathbf{u} = (u_1, u_2, u_3)$,

$$\begin{aligned} J \quad &= B_1A_h + B_2I_h(t) + B_3I_v(t) + \frac{1}{2}(W_1u_1^2(t) + W_2u_2^2(t) + W_3u_3^2(t)) \\ &\geq \frac{1}{2}(W_1u_1^2(t) + W_2u_2^2(t) + W_3u_3^2(t)) \\ &\geq \frac{1}{2}(W_1u_1^2(t) + W_2u_2^2(t) + W_3u_3^2(t)) - \eta_2 \qquad \text{since} \quad W_1u_1 - W_1 \leq 0 \\ &\geq min(\frac{1}{2}W_1, \frac{1}{2}W_2, \frac{1}{2}W_3)(u_1^2 + u_2^2 + u_3^2) - W_1 \\ &\geq \eta_1 \parallel |\mathbf{u}| \parallel^2 - \eta_2, \qquad \text{where} \quad \eta_2 = min(\frac{1}{2}W_1, \frac{1}{2}W_2, \frac{1}{2}W_3), \eta_1 = W_1, \epsilon = 2. \end{aligned}$$

This inequality indicates that the objective function J grows at least quadratically with respect to the control variables, ensuring that J is convex.The existence of an optimal control is implied by the convexity of J and the boundedness of the state variables.

Lastly, using the Calculus of Variations' Direct Method, we determine that the ideal control $\mathbf{u}^*$ that minimizes the objective function J exists within the closed and convex control set Ω. Therefore, the existence of an optimal control for Eq. (20) subject to system of Eq. (19) is established.

5. To establish this condition, we follow the approach outlined in [2]. Let

$$\dot{X} = GX + H(X) \tag{23}$$

where $X = [S_h, E_h, A_h, I_h, T_h, N_m, S_s, E_s, I_s, N_c]^T$,

$$G = \begin{bmatrix} -\mu & 0 & 0 & 0 & 0 & 0 & 0 & 0 & 0 & 0 \\ 0 & -\mu & 0 & 0 & 0 & 0 & 0 & 0 & 0 & 0 \\ 0 & 0 & -\mu & 0 & 0 & 0 & 0 & 0 & 0 & 0 \\ 0 & 0 & 0 & -\mu & 0 & 0 & 0 & 0 & 0 & 0 \\ 0 & 0 & 0 & 0 & -\mu & 0 & 0 & 0 & 0 & 0 \\ 0 & 0 & 0 & 0 & 0 & -\mu & 0 & 0 & 0 & 0 \\ 0 & 0 & 0 & 0 & 0 & 0 & -\mu & 0 & 0 & 0 \\ 0 & 0 & 0 & 0 & 0 & 0 & 0 & -\mu & 0 & 0 \\ 0 & 0 & 0 & 0 & 0 & 0 & 0 & 0 & -\mu & 0 \\ 0 & 0 & 0 & 0 & 0 & 0 & 0 & 0 & 0 & -\mu \end{bmatrix} \tag{24}$$

and

$$H(X) = \begin{bmatrix} \Lambda_h + \kappa_h T_h - \frac{\beta_h N_c S_h}{c_0 + \epsilon N_c}(1 - u_3(t)) \\ \frac{\beta_h N_c S_h}{c_0 + \epsilon N_c}\big(1 - u_3(t)\big) - \sigma_1 E_h - \sigma_2 E_h - u_1(t) E_h - \sigma_3 E_h \\ \sigma_1 E_h - u_1(t) A_h - \nu_h A_h \\ \sigma_2 E_h + \big(\tau \nu_h + u_1(t)\big) A_h - \gamma_h I_h - u_1(t) I_h - (\delta_h) I_h \\ \sigma_3 E_h + (\nu_h + u_1(t))(1 - \tau) A_h + u_1(t) I_h + \gamma_h I_h - \kappa_h T_h - ((1 - \rho)\delta_h) T_h \\ \lambda_m I_h \\ \Lambda_s - \frac{\beta_s N_m S_s}{m_0 + \epsilon N_m} - u_2(t) S_s \\ \frac{\beta_s N_m S_s}{m_0 + \epsilon N_m} - \sigma_s E_s - u_2(t) E_s \\ \sigma_s E_s - \delta_s I_s - u_2(t) I_s \\ \lambda_c I_s \end{bmatrix} \tag{25}$$

Representing

$$Z(X) = GX + H(X) \tag{26}$$

the second term, $H(X)$ in Eq. (26) satisfies

$$\begin{aligned} |H(X_1) - H(X_2)| \leq\ & a_1|S_{h_1} - S_{h_2}| + a_2|E_{h_1} - E_{h_2}| + a_3|A_{h_1} - A_{h_2}| + a_4|I_{h_1} - I_{h_2}| + a_5|T_{h_1} - T_{h_2}| \\ & + a_6|N_{m_1} - N_{m_2}| + a_7|S_{s_1} - S_{s_2}| + a_8|E_{s_1} - E_{s_2}| + a_9|I_{s_1} - I_{s_2}| + a_1 0|N_{c_1} - N_{c_2}| \\ \leq\ & a[|S_{h_1} - S_{h_2}| + |E_{h_1} - E_{h_2}| + |A_{h_1} - A_{h_2}| + |I_{h_1} - I_{h_2}| + |T_{h_1} - T_{h_2}| \\ & + |N_{m_1} - N_{m_2}| + |S_{s_1} - S_{s_2}| + |E_{s_1} - E_{s_2}| + |I_{s_1} - I_{s_2}| + |N_{c_1} - N_{c_2}|] \end{aligned}$$

Where $X_1 = (S_{h_1}, E_{h_1}, A_{h_1}, I_{h_1}, T_{h_1}, N_{m_1}, S_{s_1}, E_{s_1}, I_{s_1}, N_{c_1})$, $X_2 = (S_{h_2}, E_{h_2}, A_{h_2}, I_{h_2}, T_{h_2}, N_{m_2}, S_{s_2}, E_{s_2}, I_{s_2}, N_{c_2})$, and $a = max(a_i, i = 1,2,3,\ldots,10)$ which is independent of the state variables. Additionally, the inequality

$$[Z(X_1) - Z(X_2)] \leq a|X_1 - X_2|$$

holds, where $a = \sum_{i=1}^{10} a_i + \| Z \| \leq \infty$. Consequently, $Z(X)$ is uniformly Lipschitz continuous. Given the definitions of the control variables $u_1(t), u_2(t), u_3(t)$ and the constraints on the state variables $(S_h > 0, E_h \geq 0, A_h \geq 0, I_h \geq 0, T_h \geq 0, N_m \geq 0, S_s \geq 0, E_s \geq 0, I_s \geq 0, , N_c \geq 0)$, it follows that the solutions of Eq. (19) exist. This concludes the proof for condition (v).

6. In order to establish this property, we employ the Hessian matrix approach, which is defined as follow:
A function of multiple variables, $Q(x_1, x_2, x_3, \ldots, x_n)$, is classified as concave if and only if its Hessian matrix, H_m, satisfies

$$H_m(x) = \left[\frac{\partial^2 Q}{\partial x_i \partial x_j}\right] \leq 0, \quad \forall x \neq 0.$$

Similarly, the function is considered convex if and only if

$$H_m(x) = \left[\frac{\partial^2 Q}{\partial x_i \partial x_j}\right] \geq 0, \quad \forall x \neq 0.$$

Now, let $\mathcal{K}_i = \frac{1}{2}(W_1 u_1^2 + W_2 u_2^2 + W_3 u_3^2)$,

where $\mathcal{K}_i \in \mathcal{K}$. The Hessian matrix for $\mathcal{K}_i$ is given by

$$H_m = \begin{bmatrix} W_1 & 0 & 0 \\ 0 & W_2 & 0 \\ 0 & 0 & W_3 \end{bmatrix} \geq 0, \quad \text{for } W_1, W_2, W_3 \geq 0.$$

Thus, it follows that $\mathcal{K}_i$ is convex in U. Since $\mathcal{K}_i \in \mathcal{K}$ is convex in U, it implies that $\mathcal{K}$ is also convex in U, thereby satisfying condition (vi).

3.4.3 The uniqueness of Optimal Control

To establish the distinctiveness of the OC, we employ Pontryagin's Maximum Principle. For any optimal solution pair (x, u) there must exist a non-zero vector function

$$\lambda = \left(\lambda_{S_h}, \lambda_{E_h}, \lambda_{A_h}, \lambda_{I_h}\lambda_{T_h}, \lambda_{N_m}, \lambda_{S_s}, \lambda_{E_s}, \lambda_{I_s}, \lambda_{N_c}\right)$$

fulfilling a set of adjunct equations.

$$\begin{aligned} &\frac{\partial \mathcal{H}(t,x,u,\lambda)}{\partial u} = 0 && (optimality \quad condition)\\ &\lambda' = -\frac{\partial \mathcal{H}(t,x,u,\lambda)}{\partial x} && (adjoint \quad equation)\\ &\lambda(t_f) = 0 && (transversality \quad condition) \end{aligned} \tag{27}$$

Theorem 5. *Let $S_h^*, E_h^*, A_h^*, I_h^*, T_h^*, N_m^* S_s^*, E_s^*, I_m^*$ and N_c^* denote the optimal state trajectories and their associated* OC *variables (u_1^*, u_2^*, u_3^*) associated with the OCP defined by Eqs. (19) and (20). There exist co-state variables λ_i, which satisfy the adjoint system of equations, subject to the transversality conditions $\lambda_i(t_f) = 0$ in (25) for $i = 1,2,3, \ldots,10$, alongside the associated control parameters (u_1^*, u_2^*, u_3^*) as specified in Eq (28).*

Proof. The adjoint variables λ are described by the following DEs. These adjoint equations are derived by differentiating $\mathcal{H}$ in relation to the corresponding state variables $S_h, E_h, A_h, I_h, T_h, N_m, S_s, E_s, I_s$ and N_c respectively:

$$\begin{cases} \dot{\lambda}_{S_h} = -\frac{\partial \mathcal{H}}{\partial S_h} = -\left[\lambda_{S_h}\left(-\frac{\beta_h(1-u_3)N_c}{c_0+\epsilon N_c} - \mu_h\right) + \lambda_{E_h}\frac{\beta_h(1-u_3)N_c}{c_0+\epsilon N_c}\right], \\ \dot{\lambda}_{E_h} = -\frac{\partial \mathcal{H}}{\partial E_h} = -\left[\lambda_{E_h}\left(-(\sigma_1+\sigma_2+\sigma_3+u_1+\mu_h)\right) + \lambda_{A_h}\sigma_1 + \lambda_{I_h}\sigma_2 + \lambda_{T_h}\sigma_3\right], \\ \dot{\lambda}_{A_h} = -\frac{\partial \mathcal{H}}{\partial A_h} = -\left[B_1 + \lambda_{A_h}\left(-(\nu_h+u_1+\mu_h)\right) + \lambda_{I_h}\tau(\nu_h+u_1) + \lambda_{T_h}(1-\tau)(\nu_h+u_1)\right], \\ \dot{\lambda}_{I_h} = -\frac{\partial \mathcal{H}}{\partial I_h} = -\left[B_2 + \lambda_{I_h}\left(-(\gamma_h+u_1+\delta_h+\mu_h)\right) + \lambda_{T_h}(\gamma_h+u_1) + \lambda_{N_m}\lambda_m\right], \\ \dot{\lambda}_{T_h} = -\frac{\partial \mathcal{H}}{\partial T_h} = -\left[\lambda_{S_h}\kappa_h + \lambda_{T_h}\left(-\kappa_h - \left((1-\rho)\delta_h+\mu_h\right)\right)\right], \\ \dot{\lambda}_{N_m} = -\frac{\partial \mathcal{H}}{\partial N_m} = -\left[\lambda_{S_s}\left(-\frac{\beta_s S_s}{m_0+\epsilon N_m}\right) + \lambda_{E_s}\frac{\beta_s S_s}{m_0+\epsilon N_m} + \lambda_{N_m}(-\mu_m)\right], \\ \dot{\lambda}_{S_s} = -\frac{\partial \mathcal{H}}{\partial S_s} = -\left[\lambda_{S_s}\left(-\frac{\beta_s N_m}{m_0+\epsilon N_m} - (\mu_s+u_2)\right) + \lambda_{E_s}\frac{\beta_s N_m}{m_0+\epsilon N_m}\right], \\ \dot{\lambda}_{E_s} = -\frac{\partial \mathcal{H}}{\partial E_s} = -\left[\lambda_{E_s}\left(-(\sigma_s+\mu_s+u_2)\right) + \lambda_{I_s}\sigma_s\right], \\ \dot{\lambda}_{I_s} = -\frac{\partial \mathcal{H}}{\partial I_s} = -\left[B_3 + \lambda_{I_s}\left(-(\delta_s+\mu_s+u_2)\right) + \lambda_{N_c}\lambda_c\right], \\ \dot{\lambda}_{N_c} = -\frac{\partial \mathcal{H}}{\partial N_c} = -\left[\lambda_{S_h}\left(-\frac{\beta_h(1-u_3)S_h c_0}{(c_0+\epsilon N_c)^2}\right) + \lambda_{E_h}\frac{\beta_h(1-u_3)S_h c_0}{(c_0+\epsilon N_c)^2} + \lambda_{N_c}(-\mu_c)\right]. \end{cases} \tag{28}$$

With the transversality conditions

$$\lambda_i(T) = 0, \quad i \in \{S_h, E_h, A_h, I_h, T_h, N_m, S_s, E_s, I_s, N_c\}. \tag{29}$$

In assessing the optimal performance of the control set $u_i \in (0,1)$, let $S_h = S_h^*$, $E_h = E_h^*$, $A_h = A_h^*$, $I_h = I_h^*$, $T_h = T_h^*$, $N_m = N_m^*$ $S_s = S_s^*$, $E_s = E_s^*$, $I_s = I_s^*$ and $N_c = N_c^*$. Applying the optimality condition from the first equation in Eq. (28) and computing the partial derivatives of H in Eq. (22) with respect u_1, u_2 and u_3, we derive

$$\begin{aligned} \frac{\partial \mathcal{H}}{\partial u_1} &= W_1 u_1 - \lambda_{E_h} E_h - \lambda_{A_h} A_h + \lambda_{I_h}(\tau A_h - I_h) + \lambda_{T_h}\left((1-\tau)A_h + I_h\right) = 0, \\ \frac{\partial \mathcal{H}}{\partial u_2} &= W_2 u_2 - \lambda_{S_s} S_s - \lambda_{E_s} E_s - \lambda_{I_s} I_s = 0, \\ \frac{\partial \mathcal{H}}{\partial u_3} &= W_3 u_3 + \lambda_{S_h}\frac{\beta_h N_c S_h}{c_0+\epsilon N_c} - \lambda_{E_h}\frac{\beta_h N_c S_h}{c_0+\epsilon N_c} = 0 \end{aligned} \tag{30}$$

Hence, the solutions for u_1^*, u_2^* and u_3^* on the domains are given by:

$$\begin{aligned} u_1^* &= \frac{\lambda_{E_h} E_h + \lambda_{A_h} A_h + \lambda_{I_h}(I_h - \tau A_h) - \lambda_{T_h}\left((1-\tau)A_h + I_h\right)}{W_1} \\ u_2^* &= \frac{\lambda_{S_s} S_s + \lambda_{E_s} E_s + \lambda_{I_s} I_s}{W_2} \\ u_3^* &= \frac{\beta_h N_c S_h}{W_3(c_0+\epsilon N_c)}\left(\lambda_{E_h} - \lambda_{S_h}\right) \end{aligned} \tag{31}$$

Incorporating the control constraints $u_i \in (0,1)$ for $i = 1,2,3$ into the results from Eq. (31) yields

$$\begin{aligned} u_1^* &= max\left\{0, min\left(1, \frac{\lambda_{E_h} E_h + \lambda_{A_h} A_h + \lambda_{I_h} (I_h - \tau A_h) - \lambda_{T_h} ((1-\tau)A_h + I_h)}{W_1}\right)\right\} \\ u_2^* &= max\left\{0, min\left(1, \frac{\lambda_{S_S} S_S + \lambda_{E_S} E_S + \lambda_{I_S} I_S}{W_2}\right)\right\} \\ u_3^* &= max\left\{0, min\left(1, \frac{\beta_h N_c S_h}{W_3 (c_0 + \epsilon N_c)} (\lambda_{E_h} - \lambda_{S_h})\right)\right\} \end{aligned} \tag{32}$$

3.5 Non-autonomous System

The presented twenty-dimensional optimality problem is addressed through an iterative forward-backward sweep method, coupled with the fourth-order Runge–Kutta technique and executed within the MATLAB environment. This approach frames the problem as a two-point boundary value problem, encompassing state, adjoint, and the control equations, all formulated over a specific time frame in days. Given the opposing temporal directions of these systems, the state equations, which are non-autonomous, are integrated forward in time using established initial conditions and an initial estimation of control variables. Simulations were conducted using the baseline parameter values from Table 1, with $R_0 \approx 1.8017$. The combination of MDA and snail control was applied to evaluate the synergistic effect of these interventions on reducing the prevalence of infection and the basic reproduction number.

STRATEGY A: Combination of the use of MDA (u_1) and Snail Control via Molluscicide (u_2).

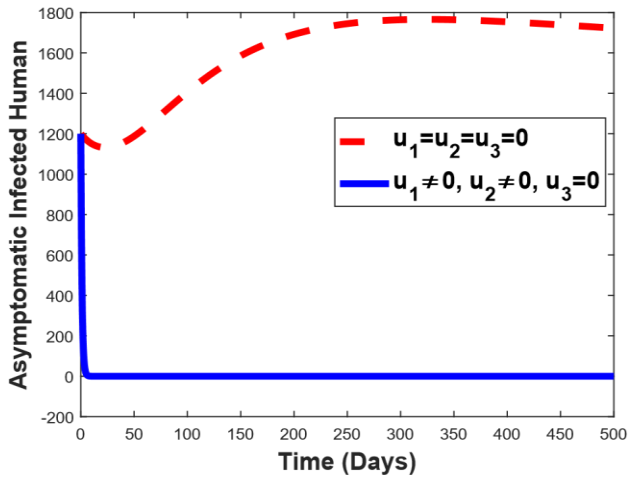

Figure 2. Asymptomatic Humans Profile

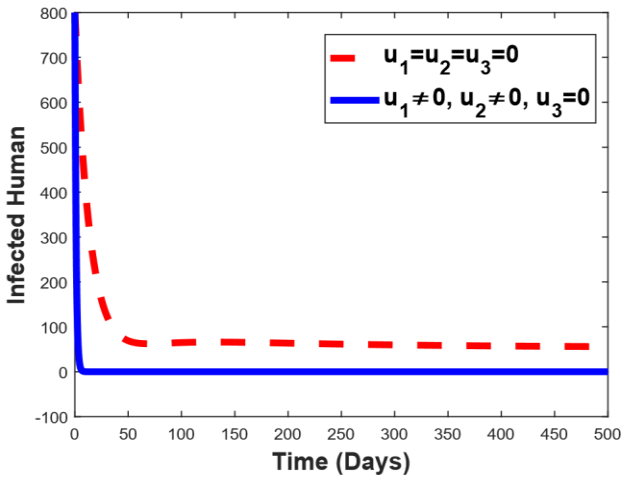

Figure 3. Infected Humans Profile

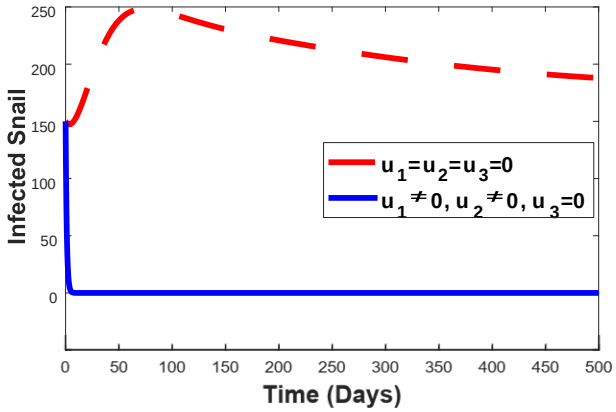

Figure 4. Infected Snails Profile

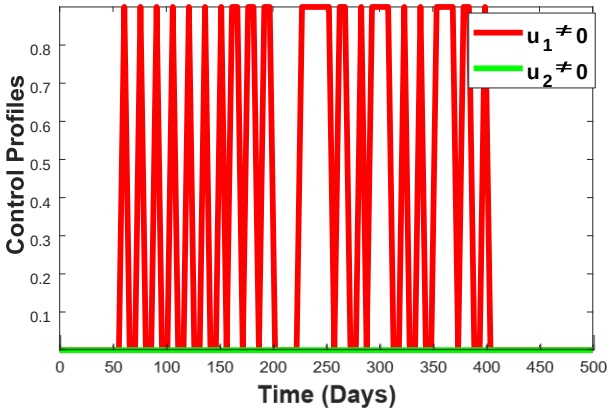

Figure 5. Control Profiles

Strategy A combines MDA (u_1) with snail control using molluscicide (u_2). The graphs clearly show that this combined approach leads to a quick and lasting drop in schistosomiasis transmission compared to the no-control case (red lines). In the Figs. 2 and 3, we see that without any intervention, the number of asymptomatic individuals and infected individuals increases and stays high. But when MDA and molluscicide are applied together, this number (blue line) drops sharply to near zero. This shows that treating infected people early can stop the disease dissemination. Furthermore, Fig. 4, which shows infected snails, reveals that without molluscicide, snail infections remain high and help keep the disease going. However, when molluscicide is used, the number of infected snails drops to zero, breaking the parasite's life cycle. Moreover,

the control profile in Fig. 5 shows how both strategies are used over time. MDA is applied in repeated strong doses, while molluscicide is used when snail populations are expected to increase. The MDA control u_1 is applied in repeated pulses throughout the simulation period, reflecting the need for ongoing treatment campaigns to maintain low infection levels. In contrast, the molluscicide control u_2 remains constant at zero after the initial period. This occurs because the optimal control solution balances intervention costs with health benefits: once the infected snail population has been sufficiently reduced (as seen in Fig. 4), the marginal benefit of continued molluscicide application does not outweigh its associated cost. The combined MDA and molluscicide strategy, the system evolves toward a disease-free steady state. Overall, this strategy demonstrates how combining MDA with snail control can significantly reduce both human and snail infections. It supports the real-world importance of using integrated interventions to eliminate schistosomiasis.

STRATEGY B: Combination of the use of Mass Drug Administration (u_1) and Water Contact Reduction (u_3).

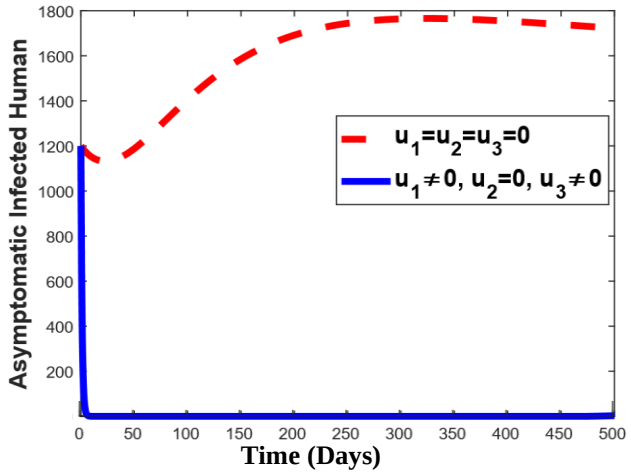

Figure 6. Asymptomatic Humans Profile

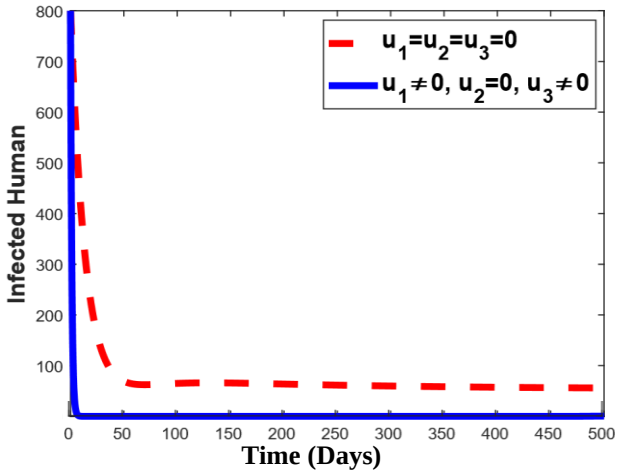

Figure 7. Infected Humans Profile

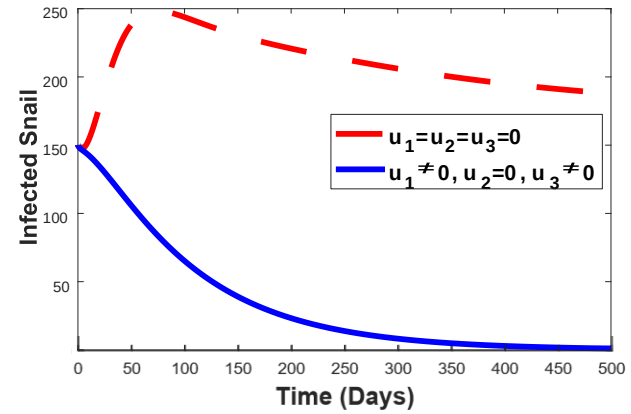

Figure 8. Infected Snails Profile

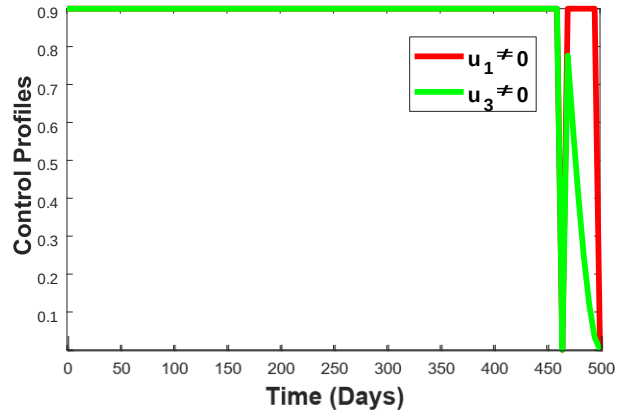

Figure 9. Control Profiles

The combination of MDA (u_1) and water contact reduction (u_3) produces a strong and consistent decline in schistosomiasis transmission across all compartments. As shown in Fig. 6, the population of asymptomatic individuals shows a sharp decline following the application of MDA, whereas it would have otherwise continued to rise significantly in the absence of intervention. This decline is sustained over time due to the reduction in water contact, which limits the chances of reinfection. Similarly, in Fig. 7 symptomatic infections collapse from several hundred to near zero, demonstrating that treating infected individuals while simultaneously promoting behavioural change can effectively reduce both the disease burden and environmental contamination. In contrast to molluscicide, which eliminates snails directly, water contact reduction gradually cuts off the parasite's reproductive cycle by lowering the number of miracidia entering the water. As a result, infected snail populations decline more slowly but still approach zero, as reflected in Fig. 8. The control profile, in Fig. 9 further illustrates this pattern: water contact reduction (u_3) is maintained at a high level throughout, suggesting sustained community engagement through education or sanitation programs, while MDA (u_1) is applied later in the intervention period to eliminate any remaining cases. Overall, this strategy highlights the effectiveness of integrating medical treatment with environmental and

behavioral interventions. This underscores the real-world importance of coordinated, long-term public health efforts that go beyond chemotherapy alone.

STRATEGY C: Combination of the Use of Snail Control via Molluscicide (u_2) and Water Contact Reduction (u_3).

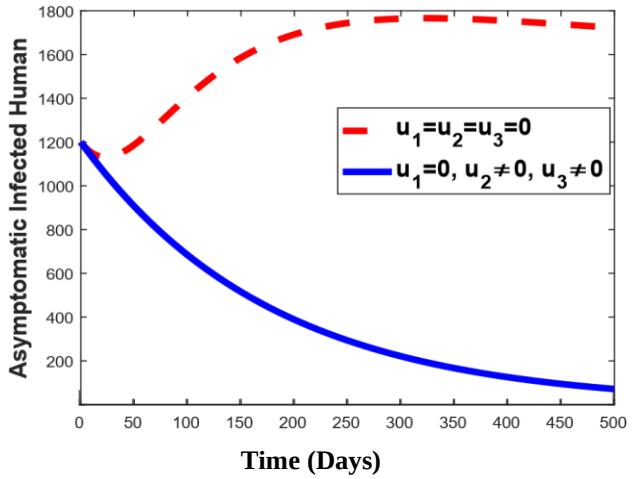

Figure 10. Asymptomatic Humans Profile

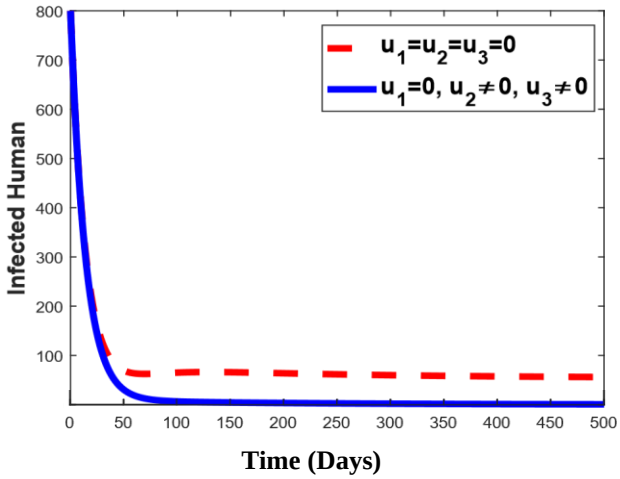

Figure 11. Infected Humans Profile

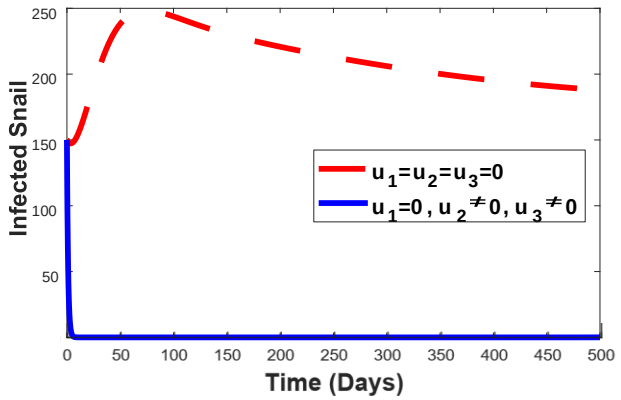

Figure 12. Infected Snails Profile

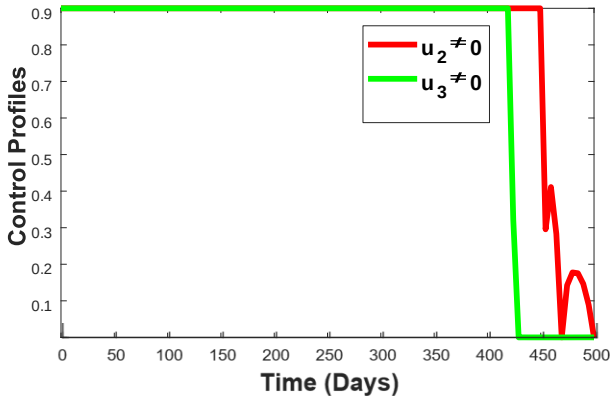

Figure 13. Control Profiles

Strategy C combines snail control using molluscicide (u_2) with sustained water contact reduction (u_3), and the results show a strong decline in schistosomiasis transmission across all compartments. In the asymptomatic human profile (see Fig. 10), infections that would have otherwise increased steadily show a gradual decline due to the combined effects of reduced snail infection and decreased human contact with contaminated water. This suggests that targeting both the intermediate host and human behaviour significantly limits new infections. Furthermore, Fig. 11 shows an even sharper drop in symptomatic cases, falling quickly from nearly 800 to almost zero. This rapid decline highlights the added value of reducing water contact alongside environmental control, as it minimizes the chances of reinfection even after successful treatment. In Fig. 12, infected snails decrease rapidly after molluscicide is introduced, while sustained water contact reduction keeps contamination levels low, preventing snail reinfection. This mirrors real-world public health strategies where chemical control is followed by education and community outreach to limit contact with snail-infested water. The control profile in Fig. 13 reveals that molluscicide (u_2) is applied early and maintained until the snail population is under control, after which water contact reduction (u_3) remains in effect to prevent resurgence. This approach reflects practical timing in real-life programs, where vector control is followed by long-term behavioural measures. Overall, Strategy C demonstrates that targeting both the environmental source of infection and human exposure leads to substantial and sustained reductions in disease transmission.

STRATEGY D: Combination of the Use of Mass Drug Administration (u_1), Snail Control via Molluscicide (u_2) and Water Contact Reduction, (u_3)

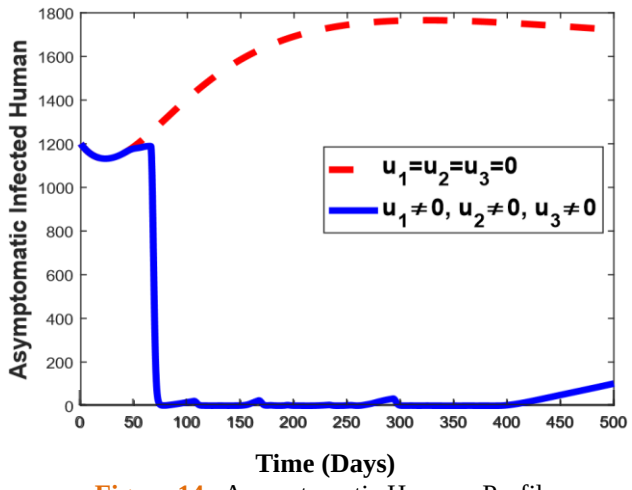

Figure 14. Asymptomatic Humans Profile

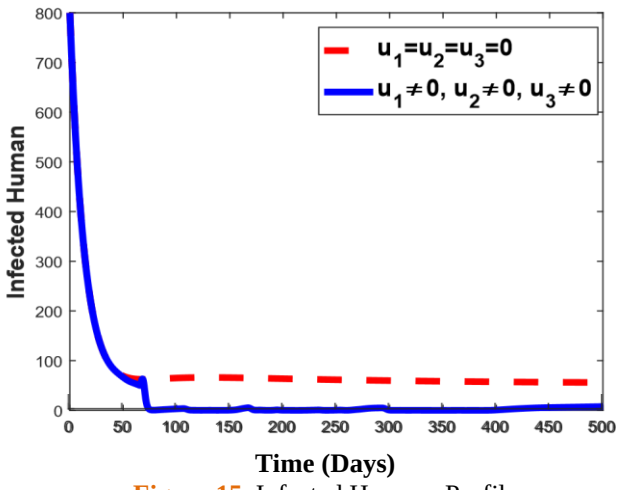

Figure 15. Infected Humans Profile

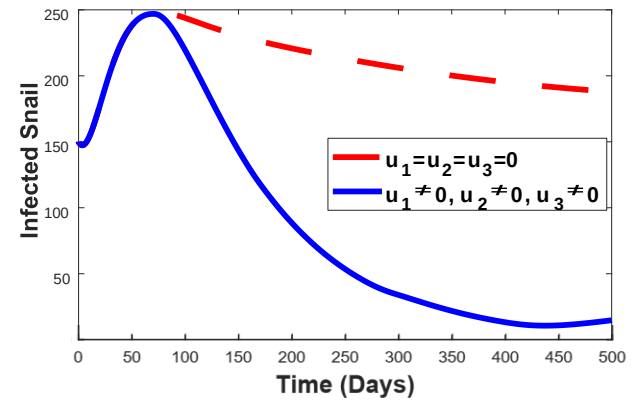

Figure 16. Infected Snails Profile

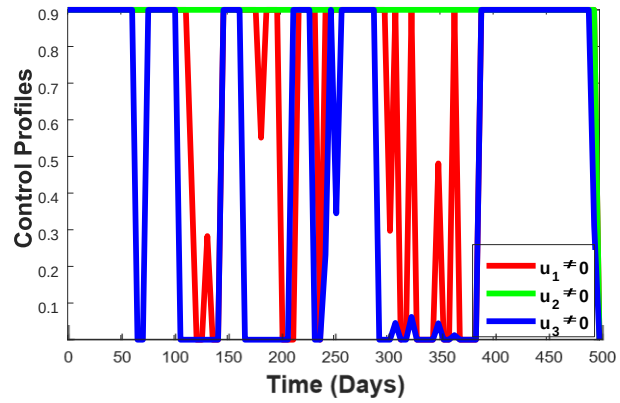

Figure 17. Control Profiles

The triple-intervention strategy, which combines the use of MDA, u_1, molluscicide to control snails (u_2), and water contact reduction (u_3), results in a significant and long-lasting reduction across all simulated cohorts in the schistosomiasis transmission model. Because of the first effect of MDA, asymptomatic human infections rapidly decrease from over 1,000 instances to almost nil, and the system heads toward a disease-free steady state as seen in Fig. 14. A slight rebound on day 250, however, suggests that molluscicide is not enough to eradicate all infected snails right away. The only way to accomplish long-term control is to continuously maintain less water contact, which lowers the chance of reinfection from polluted settings. A similar decrease in symptomatic infections is seen in Fig. 15, which decreases quickly and stays low, highlighting the importance of prompt medication treatment in minimizing disease severity and parasite contamination in aquatic environments. The number of infected snails increases temporarily in Fig. 16, but then gradually declines as a result of molluscicide and reduced human-to-environment transfer. However, over time, the infected snail population also approaches zero, consistent with convergence to the disease-free steady state. In real life, snail populations may momentarily increase after a decrease in human infection, as this early jump illustrates. Fig. 17 illustrates the control implementation, which includes consistent water contact reduction efforts (u_3) to reduce exposure, strategic molluscicide application (u_2) based on snail trends, and periodic, intense MDA campaigns (u_1) to target human reservoirs. Together, these findings demonstrate how successful a coordinated and flexible strategy involving u_1, u_2 and u_3 can halt the spread.

Table 3. Analysis of Strategies: Infections Averted, Costs, and ACER

Strategy	Initial Infected Population	Total Infection Averted	Total Cost ($)	IAR	ACER
A: u_1,u_2	2000	26074.98	672825.9351	0.0515	25.8035
B: u_1,u_3	2000	38559.88	214087.5410	0.0037	5.5521
C:u_2,u_3	2000	26706.67	1143012.3216	0.0491	42.7988
D:u_1,u_2,u_3	2000	26340.87	658891.6726	0.0505	25.0140

Table 4. Comparison of Intervention Scenarios: Total Infections Averted, Associated Costs, and Cost-Effectiveness Metrics

Strategy	Initial Infected Population	Total Infection Averted	Total Cost ($)	IAR	ICER
A: u_1,u_2	2000	26074.98	672825.9351	0.0515	-156.1023
B: u_1,u_3	2000	38559.88	214087.5410	0.0037	-117.4564
C:u_2,u_3	2000	26706.67	1143012.3216	0.0491	-134.8045
D:u_1,u_2,u_3	2000	26340.87	658891.6726	0.0505	-155.0556

Table 5. Comparative Analysis of Strategies A and D

Strategy	Initial Infected Population	Total Infection Averted	Total Cost ($)	ICER
A: u_1,u_2	2000	26074.98	672825.9351	-156.1023
D:u_1,u_2,u_3	2000	26340.87	658891.6726	-155.0556

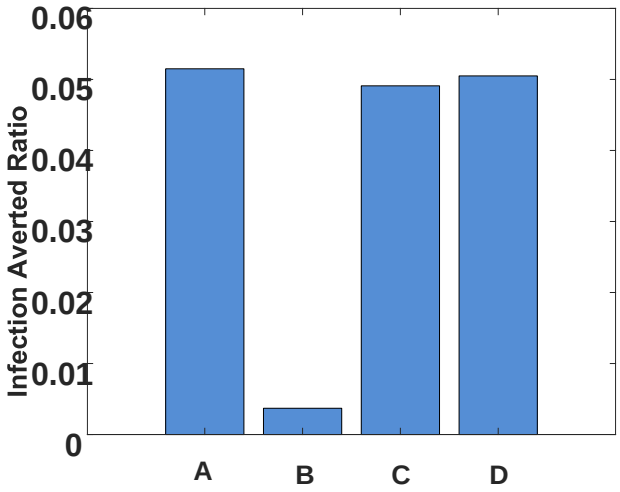

Figure 18. Visualization detailing the IAR across Strategies A, B, C, and D.

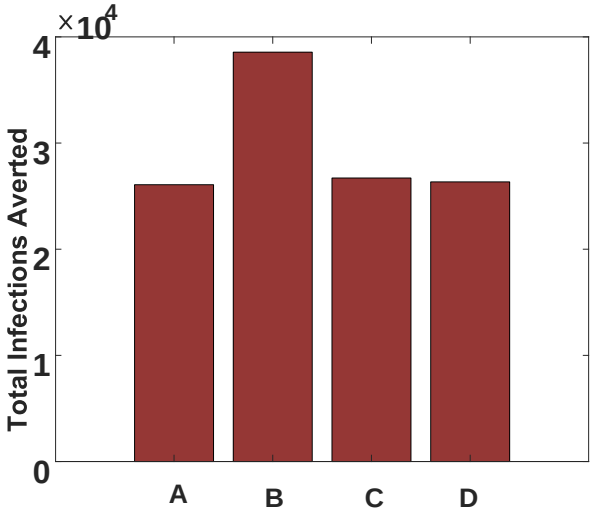

Figure 19. Visualization detailing Infection Averted for Strategies A, B, C and D

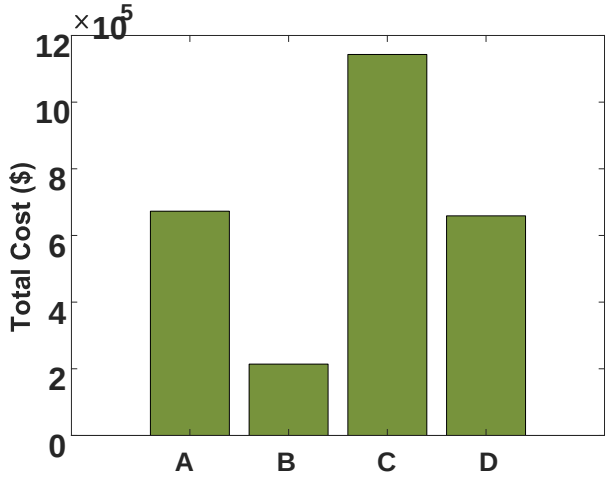

Figure 20. Total Cost of Interventions for Strategies A, B, C, and D

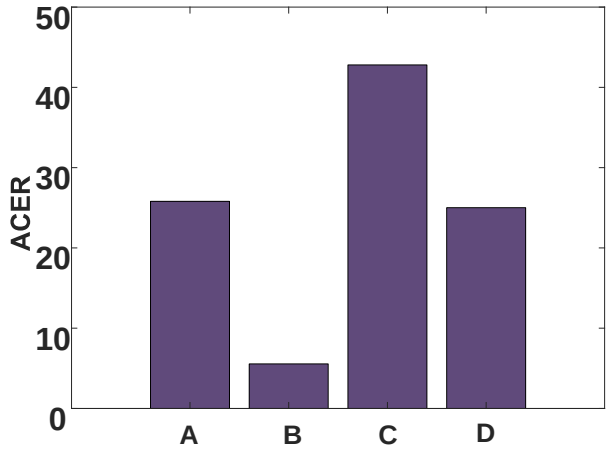

Figure 21. Average Cost-Effectiveness Ratio (ACER) for Strategies A, B, C, and D

3.6 Cost-Effectiveness Analysis

This part of the study assesses the economic efficiency of the various control strategies that have been proposed. While reducing the burden of schistosomiasis is important, it is also necessary to ensure that the resources spent on interventions provide good value for the money. Cost-effectiveness analysis helps us compare the overall cost of each strategy against the health benefits they produce, such as the reduction in infections or disease burden [42].

Infection Averted Ratio (IAR):

The Infection IAR quantifies the proportion of infections prevented by a control strategy relative to no intervention, with higher values reflecting greater effectiveness [35]. The IAR is defined as:

$$\text{IAR} = \frac{\text{Totalnumber of infection averted}}{\text{Total number of recovered}}$$

Our analysis revealed that Strategy A achieved the highest IAR of 0.0515 (see Table 4 and Fig. 19), indicating a 5.15% reduction in infections by targeting both human and snail reservoirs, effectively disrupting the parasite's life cycle. Strategy C closely followed with an IAR of 0.0491 (see Table 4 and Fig. 18), demonstrating the impact of pairing environmental interventions with behavioral measures to limit exposure. Similarly, Strategy D, the triple intervention, produced an IAR of 0.0505 (see Table 4 and Fig. 18), affirming the efficacy of integrated approaches, although the slightly lower value compared to Strategy A suggests possible diminishing returns from overlapping effects. In contrast, Strategy B had the lowest IAR of 0.0037 (see Table 4 and Fig. 18), reflecting limited impact due to the absence of direct snail control. This highlights that behavioral measures alone may be insufficient where snail populations persist. Overall, the results emphasize that incorporating snail control, whether alone or in combination, is critical to maximizing infection reduction. Strategies excluding direct vector control underperform, reinforcing the pivotal role of snail management in breaking the schistosomiasis transmission cycle.

Average Cost-Effectiveness Ratio (ACER):

The ACER assesses the cost per infection averted, serving as a key indicator of how efficiently each strategy translates investment into health gains [35]. Lower ACER values reflect more cost-efficient interventions.

$$\text{ACER} = \frac{\text{Total cost of implementing the strategy}}{\text{Total number of infections it successfully prevents}}$$

Among the evaluated strategies, Strategy B achieved the lowest ACER of 5.55 (see Table 3 and Fig. 21), which signifies it is the most cost-efficient, despite its limited impact on overall infection reduction. Its affordability stems from avoiding the direct expenses of snail control, making it an attractive option for resource-limited settings. Strategy D (the triple intervention) followed with an ACER of 25.01 (see Table 3 and Fig. 21), balancing cost with higher health benefits due to its broader approach. Similarly, Strategy A resulted in a comparable ACER of 25.80 (see Table 3 and Fig. 21), suggesting that adding water contact reduction (as in Strategy D) slightly enhances cost-effectiveness. Conversely, Strategy C had the highest ACER at 42.80 (see Table 3 and Fig. 21), portraying it as the least cost-effective, likely due to operational expenses and the absence of MDA, which limits rapid infection reduction.

Incremental Cost-Effectiveness Ratio (ICER):

The ICER evaluates the additional cost needed to avert one extra infection when shifting between strategies [35]. A negative ICER, as seen in all strategies here, signals dominance: meaning the intervention both improves health out26comes and reduces costs compared to the alternatives. It is defined as

$$\text{ICER} = \frac{e_1 - e_2}{e_3 - e_4},$$

where e_1 is the total cost with control, e_2 is the total cost without control, e_3 is the total number of infections without control and e_4 is the total number of infections with control.

Strategy A yields the lowest ICER at -156.10 (see Table 4), making it the most cost-saving and health-effective option. This underscores its suitability for policies aiming to maximize infection reduction while minimizing costs. Strategy D (the triple intervention) followed closely with an ICER of -155.06 (see Table 4), offering substantial savings and health benefits, particularly valuable for long-term control and transmission interruption. Strategy C recorded an ICER of -134.80 (see Table 4), reflecting lesser cost-effectiveness due to operational costs and the lack of direct human treatment. Lastly, Strategy B showed the least negative ICER at -117.46 (see Table 4), aligning with earlier metrics that indicate it is economically favorable but less impactful in reducing infections. As presented in Table 5, Strategy D (which integrates MDA, snail control via molluscicide, and water contact reduction) demonstrates superior performance compared to Strategy A (which includes only MDA and snail control). Specifically, Strategy D averts a slightly higher number of infections while also incurring a lower total cost. This suggests that the addition of water contact reduction not only enhances health impact but also improves economic efficiency. Although

both strategies have similarly favorable ICER values, the marginal gains in both cost savings and infections averted make Strategy D the more desirable option for comprehensive schistosomiasis control.

4. CONCLUSION

This study demonstrates that an integrated approach combining MDA, snail control via molluscicide, and water-contact reduction is substantially more effective at suppressing schistosomiasis transmission than any single intervention. Our optimal control analysis and numerical simulations confirm that targeting multiple transmission pathways simultaneously is required to lower the disease's basic reproduction number below one and achieve long-term control. While MDA alone can temporarily reduce prevalence, it often fails to sustain low transmission levels, especially in the presence of untreated environmental reservoirs and snail populations. Importantly, the inherently non-linear feedback between human and snail hosts means that these interventions interact synergistically. Treating human infections while simultaneously reducing snail populations and limiting exposure to infested water amplifies the overall impact of control measures. Although some field studies have observed limited short-term gains from adding snail control to MDA, our results suggest that sustained, large-scale deployment of all the three interventions is essential for durable reductions in infection. Incorporating cost-effectiveness analysis further strengthens the case for integrated strategies. Our evaluation using standard health economic metrics including the IAR, ACER, and ICER revealed that Strategy B achieved the highest number of infections averted while also incurring the lowest total cost among the evaluated strategies. Notably, all ICER values were negative, indicating economic dominance: the integrated strategies were both more effective and less costly than the no-control baseline. These findings offer clear policy direction. Schistosomiasis continues to pose a major challenge in numerous regions where it is endemic, and WHO’s outlined plan to eradicate neglected tropical diseases by the year 2030 emphasizes the need for integrated, multi-sectoral interventions. We strongly recommend that health authorities and governments in endemic settings adopt and sustain comprehensive control programs that combine pharmacological treatment with environmental management and behavioural change. Such coordinated strategies not only maximize health gains but also ensure efficient use of limited public health resources.

Author Contributions

A. S. Afolabi: Conceptualization, Data curation, Formal Analysis, Investigation, Methodology, Project Administration, Resources, Software, Supervision, Validation, Visualization, Writing - Original Draft, Writing - Review and Editing. J. C. Orji: Data Curation, Formal Analysis, Investigation, Methodology, Project Administration, Resources, Software, Validation, Visualization, Writing - Original Draft, Writing - Review and Editing. All authors discussed the results and contributed to the final manuscript.

Funding Statement

This research did not obtain financial backing from any public, commercial, or non-profit funding organizations.

Acknowledgment

The authors sincerely appreciate the valuable comments and constructive suggestions provided by the reviewers.

Declarations

The authors declare no competing interest.

Declaration of Generative AI and AI-assisted technologies

Generative AI tools were used solely for language refinement (grammar, spelling, and clarity). The scientific content, analysis, interpretation, and conclusions were developed entirely by the authors. The authors reviewed and approved all final text.

REFERENCES

[1] A. V. Diaz, M. Walker and J. P. Webster, "REACHING WHO ELIMINATION TARGETS FOR SCHISTOSOMIASIS: A ONE HEALTH PERSPECTIVE," *Phil. Trans. R. Soc. B,* no. 378, 2023. doi: https://doi.org/10.1098/rstb.2022.0274

[2] WHO, "SCHISTOSOMIASIS (BILHARZIA)," 2024. [Online]. Available: https://www.who.int/health-topics/schistosomiasis

[3] WHO NTD Programme, "SCHISTOSOMIASIS AND SOIL-TRANSMITTED HELMINTHIASES: PROGRESS REPORT 2023," 2024. [Online]. Available: https://www.who.int/publications/i/item/WHO-WER9948-707-717.

[4] S. H. Sokolow *et al*., "GLOBAL ASSESSMENT OF SCHISTOSOMIASIS CONTROL OVER THE PAST CENTURY," *PLOS Negl Trop Dis,* p. e0004794, 2016. doi: https://doi.org/10.1371/journal.pntd.0004794

[5] L. Trippler *et al*., "IMPACT OF CHEMICAL SNAIL CONTROL IN PEMBA, TANZANIA," *Parasites & Vectors,* no. 17, p. 489, 2024.

[6] S. Summers, "EPIDEMIOLOGY AND GENETIC ANALYSIS OF PRAZIQUANTEL TREATMENT RESPONSE OF SCHISTOSOMA MANSONI IN PRESCHOOL-AGED CHILDREN IN UGANDA," Doctoral dissertation, London School of Hygiene & Tropical Medicine, 2025.

[7] L. C. Anderson, E. S. Loker and H. J. Wearing, "MODELING SCHISTOSOMIASIS TRANSMISSION: THE IMPORTANCE OF SNAIL POPULATION STRUCTURE," *Parasites & Vectors,* no. 14, pp. 1-14, 2021. doi: https://doi.org/10.1186/s13071-021-04587-8

[8] J. Toor *et al*., "ACHIEVING ELIMINATION AS A PUBLIC HEALTH PROBLEM FOR SCHISTOSOMIASIS," *J. Infect. Dis.,* no. 221(Suppl 5), p. S525–S530, 2020. doi: https://doi.org/10.1093/infdis/jiz609

[9] Q. Huang *et al*., "SCHISTOSOMA TRANSMISSION IN A DYNAMIC SEASONAL ENVIRONMENT," *J. Infect. Dis.,* no. 225(6), p. 1050–1061, 2022.

[10] E. Y. Li *et al*., "IMPROVING PUBLIC HEALTH CONTROL OF SCHISTOSOMIASIS WITH MODIFIED WHO STRATEGY," *Lancet Global Health,* no. 7(10), p. e1414–e1422, 2019. doi: https://doi.org/10.1016/S2214-109X(19)30346-8

[11] E. Nyandwi *et al*., "MODELING SCHISTOSOMIASIS SPATIAL RISK DYNAMICS IN RWANDA," *Scientific Reports,* no. 10(1), p. 19276, 2020.

[12] A. G. Buchwald *et al*., "HUMAN MOBILITY ASSOCIATED WITH RISK OF SCHISTOSOMA JAPONICUM INFECTION IN SICHUAN, CHINA," *Am. J. Epidemiol.,* no. 190(7), p. 1243–1252, 2021. doi: https://doi.org/10.1093/aje/kwaa292

[13] A. G. Djirmay *et al*., "CHEMICAL CONTROL OF SNAIL VECTORS AS AN INTEGRATED PART OF ELIMINATION STRATEGY," *Trop. Med. Infect. Dis.,* no. 9(9), p. 222, 2024. doi: https://doi.org/10.3390/tropicalmed9090222

[14] M. B. Adediran, A. Adesida, O. O. Ezekiel, P. C. Irabor, B. M. Babalola and O. T. Oyeyemi, "FROM TREATMENT TO PREVENTION: REIMAGINING SCHISTOSOMIASIS CONTROL THROUGH WASH AND ENVIRONMENTAL MANAGEMENT.," *Pathogens and Global Health,* pp. 1-17, 2025. doi: https://doi.org/10.1080/20477724.2025.2603235

[15] N. C. Lo *et al*., "IMPACT AND COST-EFFECTIVENESS OF SNAIL CONTROL," *Proc. Natl. Acad. Sci.,* no. 115(4), p. E584–E591, 2018.

[16] H. R. J. KuraK., T. J. E and A. R. M., "WHAT IS THE IMPACT OF ACQUIRED IMMUNITY ON THE TRANSMISSION OF SCHISTOSOMIASIS AND THE EFFICACY OF CURRENT AND PLANNED MASS DRUG ADMINISTRATION PROGRAMMES?," *PLOS Neglected Tropical Diseases,* vol. 15, no. 12, 2021. doi: https://doi.org/10.1371/journal.pntd.0009946

[17] J. E. Truscott, D. Gurarie, R. Alsallaq, J. Toor, N. Yoon, S. Farrell, H. C. Turner, A. E. Phillips, H. O. Aurelio, J. Ferro, C. H. King and R. M. Anderson, "A COMPARISON OF TWO MATHEMATICAL MODELS OF THE IMPACT OF MASS DRUG ADMINISTRATION ON THE TRANSMISSION AND CONTROL OF SCHISTOSOMIASIS," *Epidemics,* vol. 18, pp. 29-37, 2017. doi: https://doi.org/10.1016/j.epidem.2017.02.003

[18] E. Kanyi, A. S. Afolabi and N. O. Onyango, "MATHEMATICAL MODELING AND ANALYSIS OF SCHISTOSOMIASIS," *Journal of Applied Mathematics,* no. 2021(1), p. 6653796, 2021. doi: https://doi.org/10.1155/2021/6653796

[19] C. Castillo-Chavez, Z. Feng and W. Huang, "ON THE COMPUTATION OF R0 AND ITS ROLE ON GLOBAL STABILITY," 2001. doi: https://doi.org/10.1007/978-1-4757-3667-0_13

[20] M. T. Vaillant *et al*., "DIAGNOSTIC TESTS FOR SCHISTOSOMA INFECTION: SYSTEMATIC REVIEW," *Lancet Microbe,* 2024.

[21] D. S. Brown, Freshwater snails of Africa and their medical importance, CRC Press, 1994. doi: https://doi.org/10.1201/9781482295184

[22] R. M. Anderson, Infectious diseases of humans: dynamics and control, Oxford University Press, 1991. doi: https://doi.org/10.1093/oso/9780198545996.001.0001

[23] I. D. Onisanwa *et al*., "DETERMINANTS OF LIFE EXPECTANCY IN NIGERIA," *Tanzania Economic Review,* no. 14(1), 2024.

[24] WHO, "NIGERIA DATA," 2023.

[25] W. Xu, C. Zhao, X. Pan, X. He, X. Liu, J. Hou and J. Pang, "TRANSMISSION ROUTES AND A NEW FRESHWATER CRUSTACEAN HOST FOR INFECTIOUS PRECOCITY VIRUS (IPV).," *Transboundary and Emerging Diseases,* vol. 1, p. 3950107, 2023. doi: https://doi.org/10.1155/2023/3950107

[26] H.-A. A. Dokmak, O. A. Hammam and A. M. Ibrahim, "IMPACT OF SCHISTOSOMA SP. INFECTION ON SNAILS," *Acta Parasitologica,* no. 69(1), p. 648–663, 2024. doi: https://doi.org/10.1007/s11686-023-00760-4

[27] D. Buonfrate, T. C. A. Ferrari, A. A. S. J. R. Adegnika and F. G. & Gobbi, "HUMAN SCHISTOSOMIASIS. 405(10479),," *The Lancet,*, vol. 405, no. 10479, pp. 658-670, 2025. doi: https://doi.org/10.1016/S0140-6736(24)02814-9

[28] F. Allan *et al*., "SNAIL-RELATED CONTRIBUTIONS FROM THE SCHISTOSOMIASIS CONSORTIUM…," *Am. J. Trop. Med. Hyg.*, no. 103(1 Suppl), p. 66, 2020.

[29] P. Makaula *et al*., "IMPLEMENTATION AND EFFECTIVENESS OF MASS DRUG ADMINISTRATION IN MALAWI," *BMC Health Services Research,* no. 22(1), p. 517, 2022.

[30] N. Chanhanga *et al*., "THE IMPACT OF TARGETED TREATMENT AND MASS DRUG ADMINISTRATION…," *Infection and Drug Resistance,* p. 2453–2466, 2023.

[31] A. W. Cheever *et al*., "EXPERIMENTAL MODELS OF SCHISTOSOMA MANSONI INFECTION," *Mem. Inst. Oswaldo Cruz,* no. 97, p. 917–940, 2002. doi: https://doi.org/10.1590/S0074-02762002000700002

[32] N. Ø. C. F. Frandsen, "AN INTRODUCTORY GUIDE TO THE IDENTIFICATION OF CERCARIAE…," 1984.

[33] C. P. de Souza *et al*., "A STOCK OF INFECTED SNAILS FOR MASS BREEDING," *Mem. Inst. Oswaldo Cruz,* no. 80(1), p. 55–61, 1985. doi: https://doi.org/10.1590/S0074-02761985000100009

[34] M. E. J. Woolhouse *et al*., "ACQUIRED IMMUNITY AND EPIDEMIOLOGY OF SCHISTOSOMA HAEMATOBIUM," *Nature,* no. 351(6329), p. 757–759, 1991. doi: https://doi.org/10.1038/351757a0

[35] G. W. Esch, L. A. Curtis and M. A. Barger, "A PERSPECTIVE ON THE ECOLOGY OF TREMATODE COMMUNITIES IN SNAILS," *Parasitology,* no. 123(7), p. 57–75, 2001. doi: https://doi.org/10.1017/S0031182001007697

[36] A. S. Afolabi and M. Miswanto, "MATHEMATICAL MODELING, OPTIMAL CONTROL AND COST-EFFECTIVENESS ANALYSIS OF DIPHTHERIA…," *Jambura Journal of Biomathematics (JJBM),* no. 190(6), p. 88–108, 2025. doi: https://doi.org/10.37905/jjbm.v6i2.30851

[37] R. L. Mester, R. C. A. and K. Lange, "DIFFERENTIAL METHODS FOR ASSESSING SENSITIVITY IN BIOLOGICAL MODELS.," *PLoS computational biology,* vol. 18, no. 6, p. e1009598, 2022. doi: https://doi.org/10.1371/journal.pcbi.1009598

[38] O. Sharomi and T. Malik, "OPTIMAL CONTROL IN EPIDEMIOLOGY," *Annals of Operations Research,* no. 251, p. 55–71, 2017. doi: https://doi.org/10.1007/s10479-015-1834-4

[39] K. W. Blayneh, "UNIFORM PERSISTENCE AND BACKWARD BIFURCATION OF VERTICALLY TRANSMITTED VECTOR-BORNE DISEASES.," *Research in Mathematics,* vol. 10, no. 1, p. 2264581, 2023. doi: https://doi.org/10.1080/27684830.2023.2264581

[40] A. A. Momoh and A. Fügenschuh, "OPTIMAL CONTROL OF INTERVENTION STRATEGIES AND COST-EFFECTIVENESS FOR ZIKA MODEL," *Operations Research for Health Care,* no. 18, p. 99–111, 2018. doi: https://doi.org/10.1016/j.orhc.2017.08.004

[41] A. I. Abioye *et al*., "OPTIMAL CONTROL ON A MATHEMATICAL MODEL OF MALARIA," *Sci. Bull., Series A: Appl Math Phy,* no. 82(3), p. 177–190, 2020.

[42] J. Orji, T. Yusuf and A. Afolabi, " INTEGRATED MALARIA CONTROL: IMPACTS OF VACCINATION AND COMBINED INTERVENTIONS ON DISEASE DYNAMICS.," *Model. Earth Syst. Environ,* vol. 11, p. 399, 2025. doi: https://doi.org/10.1007/s40808-025-02522-9

[43] P. Muennig and M. Bounthavong, Cost-effectiveness analysis in health: a practical approach, Wiley, 2016.

[44] Centers for Disease Control and Prevention, "CDC - DPDX - SCHISTOSOMIASIS INFECTION," 2019. [Online]. Available: https://www.cdc.gov/dpdx/schistosomiasis/index.html.

[45] J. E. T. Grimes *et al*., "THE ROLES OF WATER, SANITATION AND HYGIENE IN REDUCING SCHISTOSOMIASIS," *Parasites & Vectors,* no. 8, pp. 1-16, 2015. doi: https://doi.org/10.1186/s13071-015-0766-9

[46] S. H. Sokolow *et al*., "REDUCED TRANSMISSION AFTER RESTORATION OF NATIVE RIVER PRAWN," *Proc. Natl. Acad. Sci.,* no. 112(31), p. 9650–9655, 2015. doi: https://doi.org/10.1073/pnas.1502651112

[47] R. S. Barsoum, "HUMAN SCHISTOSOMIASIS," *Reference Module in Biomedical Sciences,* 2014. doi: https://doi.org/10.1016/B978-0-12-801238-3.00255-5

[48] L. C. Anderson, E. S. Loker and H. J. Wearing, "MODELING SCHISTOSOMIASIS TRANSMISSION: THE IMPORTANCE OF SNAIL POPULATION STRUCTURE," *Parasites & Vectors,* no. 14, pp. 1-14, 2021. doi: https://doi.org/10.1186/s13071-021-04587-8